sustainability

MDPI

Review

A Review of Thermochromic Materials for Passive Adaptive Solar Regulation in Buildings: Mechanisms, Performance and Applications

Cong Chen [1], Kai Huang [2], Yongkang Gui [2], Xiao Huang [3] and Caixia Wang [2,*]

[1] National Science Library (Wuhan), Chinese Academy of Sciences, No. 25, Xiaohongshan West, Wuchang District, Wuhan 430071, China
[2] School of Civil Engineering and Architecture, Wuhan University of Technology, No. 122 Luoshi Road, Wuhan 430070, China
[3] School of Resources, Environment and Materials, Guangxi University, No. 100 Daxue East Road, Nanning 530004, China
* Correspondence: caixia.wang@whut.edu.cn

Abstract

Thermochromic materials (TCMs) have attracted increasing attention as passive adaptive materials for solar regulation in buildings because they can reversibly change their optical properties in response to temperature without external energy input. Owing to this temperature-triggered optical modulation, they have been widely investigated for smart windows, temperature indicators, anti-counterfeiting labels, and flexible devices. In recent years, representative systems such as VO_2-based materials, polymers, hydrogels, and organic–inorganic hybrids have shown steady progress, especially in transition-temperature tuning, spectral selectivity, and cycling stability. This review summarizes the main classes of TCMs as well as their color-changing mechanisms, preparation methods, and performance-regulation strategies, with an emphasis on building energy efficiency and passive solar regulation. Typical applications and current bottlenecks are also discussed, including response speed, durability, environmental compatibility, and large-scale manufacturing. Finally, several practical directions for future work are highlighted, particularly low-cost synthesis, multifunctional integration, and application-oriented material design.

Keywords: thermochromic materials; passive solar regulation; building energy efficiency

1. Introduction

Amid growing energy pressure and increasingly urgent carbon-reduction targets, improving building energy efficiency has become a major priority worldwide. Buildings account for a substantial share of global energy use, and heating, ventilation, and air-conditioning (HVAC) systems remain one of the main contributors to operational energy demand [1]. In this context, passive regulation of solar radiation through functional materials has attracted increasing attention as a practical way to reduce cooling and heating loads while maintaining indoor thermal and visual comfort. Among temperature-responsive materials, thermochromic materials (TCMs) are particularly appealing because they can adjust their optical properties automatically with temperature, without relying on external power input or complex control systems [2–6]. Depending on the material system, this response may appear as a change in visible color, transmittance, reflectance, or near-infrared modulation, which makes TCMs especially promising for smart windows, exterior coatings, temperature indicators, anti-counterfeiting labels, and other intelligent devices [7–10].

Check for updates

Academic Editor: Antonio Caggiano

Received: 14 February 2026
Revised: 30 March 2026
Accepted: 13 April 2026
Published: 22 April 2026

Copyright: © 2026 by the authors. Licensee MDPI, Basel, Switzerland. This article is an open access article distributed under the terms and conditions of the Creative Commons Attribution (CC BY) license.

Current research mainly focuses on two representative classes of TCMs: inorganic systems, especially vanadium dioxide (VO_2), and organic systems such as thermo-responsive hydrogels. VO_2 is one of the most widely studied inorganic thermochromic materials because it undergoes a metal–insulator transition near 68 °C, accompanied by a marked change in infrared optical properties, making it highly relevant for smart windows and energy-saving coatings [11–14]. However, its relatively high transition temperature and limited visible transmittance still restrict practical use under ambient conditions [15]. By contrast, hydrogels regulate light through changes in volume, refractive index, and scattering behavior, which gives them advantages in flexibility and tunability [16,17]. Their main limitations are relatively slow response, weak mechanical strength, and insufficient long-term stability.

Thermochromic behavior is not limited to synthetic materials. Some natural minerals also show temperature-dependent color change. For example, ruby can change from red to green on heating and return to red on cooling, a phenomenon related to temperature-dependent changes in the electronic transitions of transition-metal ions in the lattice [18]. At the same time, advances in nanotechnology and materials chemistry have greatly expanded the design space of TCMs and improved control over composition and microstructure.

For building applications, thermochromic coatings or films can be applied to walls, roofs, and glass to regulate solar heat gain under changing environmental conditions [19]. Smart windows based on these materials can adjust visible transmittance and near-infrared blocking ability with temperature, helping balance energy saving, glare control, and indoor comfort [20]. Despite this progress, practical use is still limited by several factors, including the high transition temperature of VO_2, the difficulty of balancing visible transparency with color performance, the poor durability of some organic systems, and the cost or environmental concerns associated with certain material formulations.

This review summarizes the main material systems, working mechanisms, preparation methods, performance evaluation approaches, and representative applications of TCMs, with particular attention to building energy efficiency and passive solar regulation. It also discusses the main challenges that continue to limit practical deployment and highlights directions for future research.

2. State of the Art

2.1. Research Domains and Interdisciplinary Characteristics

Research on TCMs is inherently interdisciplinary, involving materials science, chemistry, physics, optics, and building engineering. Earlier studies were largely concerned with material discovery, phase-transition or molecular mechanisms, and basic optical characterization. As the field has developed, increasing attention has been given to application-oriented questions such as transition-temperature tuning, spectral selectivity, durability, processability, and compatibility with coatings, glazing, and flexible substrates. Nanostructuring, composite design, and multifunctional integration have all contributed to this shift, but the extent of performance improvement remains strongly dependent on material class, morphology, and test conditions.

2.2. Temporal Trends and the Evolution of Research Hotspots

The literature shows a clear shift from mechanism-focused studies to application-oriented optimization. Earlier work was mainly centered on synthesis, structure–property relationships, and fundamental thermochromic behavior. More recent studies have paid greater attention to lowering transition temperature, balancing visible transmittance with solar modulation, improving cycling stability, and adapting fabrication routes for films, coatings, and composite systems [21]. Sustainability, environmental compatibility, and

scale-up feasibility have also become more visible themes, particularly in work related to building envelopes and smart-window applications. Because this review was not designed as a formal bibliometric study, quantitative publication statistics are not reported here.

2.3. Research Challenges and Future Prospects

Environmental compatibility remains an important issue in thermochromic-material research. Some systems still rely on metal-containing compounds, volatile organic solvents, or other components that may raise concerns during synthesis, processing, use, or disposal. In addition to environmental issues, practical application is also limited by transition-temperature regulation, durability, large-scale manufacturability, and cost control. Future work should therefore place more emphasis on low-toxicity material design, stable long-term performance, and scalable preparation routes. These broader challenges, especially those related to green design and life-cycle considerations, will be discussed further in the following sections.

3. Classification and Mechanisms of Color Change in TCMs

3.1. Classification of TCMs

TCMs are a class of functional materials that respond to temperature changes by altering their color or optical properties. When this process is reversible, such materials are especially attractive for practical applications ranging from smart windows to sensors and temperature indicators [22]. Based on composition and functional characteristics, TCMs are generally classified into inorganic TCMs, organic TCMs, and several emerging or specialized systems. This classification is useful not only in terms of material chemistry, but also because different classes usually correspond to different application needs, as detailed in Table 1.

Inorganic TCMs mainly include metal iodides, double salts, transition-metal compounds, metal alloys, and metal chlorides. These materials usually show better thermal stability, durability, and light resistance, which makes them more suitable for long-service applications such as smart windows, exterior coatings, and other building-related systems.

By contrast, organic TCMs cover a wider range of compounds, including spiropyrans, anthocyanins, triarylmethanes, substituted ethylene derivatives, and organic complexes. Their main advantages are tunable colors, lower switching temperatures, high sensitivity, flexibility, and relatively low cost. These features make them attractive for indicators, textiles, flexible devices, and other applications where vivid color change and mild operating conditions are more important than long-term thermal resistance. However, their lower stability at elevated temperatures can limit broader use.

In addition, other specialized classes of TCMs, such as quantum dots, plasmonic structures, photonic crystals, conjugated polymers, Schiff bases, and liquid crystals, exhibit distinctive physical and chemical properties. These systems are particularly valuable when high optical tunability, structural color effects, or strong sensitivity are required. Therefore, the classification of TCMs should also be understood from an application-oriented perspective: the same thermochromic mechanism may be advantageous in one scenario but less suitable in another, depending on the required operating temperature, optical contrast, reversibility, durability, and processability [23].

Table 1. Mechanisms of color change in TCMs [23].

Material Type		Application Scope	Material Characteristics				
			Durability and Stability	Color Range	Ductility	Reaction Speed	Controllability
Inorganic TCM	Crystal Transformation	Production and processing of materials	✔✔	NR	✔	✔✔	✔✔
	Loss or Gain of Crystal Water	Controlling and managing moisture in buildings	✔	NR	✔	✔	✔✔
	Electron Transfer	Smart Homes, security systems and lighting control	✔✔	NR	✔	✔✔	✔✔
	Ligand Geometric Change	Modulation of optical, magnetic and electrical properties of materials	✔✔	✔	✔	✔	✔✔
Organic TCM	pH Change Mechanism	Indoor environmental control	✔✔	✔	✔	✔	✔✔
	Electron Gain/Loss Mechanism	Smart windows and building facades, thermal and solar control	✔	NR	✔	✔✔	✔✔
Other TCM	Quantum Dots	Curtains, partitions, door and window glass	✔✔	✔	✔	✔	✔✔
	Plasmonics	Temperature-sensitive coatings, smart window glass	✔	✔	✔	✔	✔✔
	Photonic Crystals	Optical sensors, interior decorative materials	✔	✔✔	✔	✔	✔✔
	Conjugated Polymers	Indoor lighting, decorative materials	✔	✔✔	✔	✔	✔✔
	Schiff Bases	Indoor lighting, decorative materials	✔	NR	✔	✔	✔
	Origami Structure	Curtains, door and window glass	NR	NR	✔✔	NR	NR
	Liquid Crystals	Smart glass, Liquid Crystal Displays	✔✔	✔	✔✔	✔	✔

Note: "✔" indicates basic compliance, "✔✔" indicates strong compliance, "NR" indicates not reported.

3.2. Reversible Organic TCMs

Organic reversible TCMs can be categorized into two main types based on their composition. The first type consists of single-component compounds that undergo compositional or structural changes upon heating, exhibiting thermochromic behavior. These materials can be directly used as TCMs.

In contrast, the second type comprises multi-component composites containing one or more colored or colorless compounds. These compounds do not exhibit color change on their own; however, when combined with suitable partners, they undergo chemical or physical interactions that generate thermochromic effects. As a result, multi-component composites display more complex thermochromic behavior.

Classified according to organic chemical nomenclature, organic reversible TCMs comprise a diverse range of compounds, such as triarylmethane phthalates, indole phthalates, fluorescent agents, triphenylmethane derivatives, spiropyran derivatives, spirocycles, dianthrones, α-naphthoquinone derivatives, polymers (e.g., polyethylene, polysilane, polygermanene, polythiophene), and biomacromolecules.

3.2.1. pH-Dependent Color-Changing Mechanism

The color-changing mechanism in certain organic TCMs arises from acid–base indicators combined with one or more fusible carboxylic acids and amine compounds. Upon

temperature variations, these fusible compounds induce pH shifts, leading to melting or solidification. Consequently, changes in the acid–base environment or temperature cause transformations in molecular structures, resulting in reversible color changes in the material.

3.2.2. Electron Transfer Mechanisms

Organic reversible TCMs employing this color-changing mechanism typically consist of three components, namely an electron donor, an electron acceptor, and a solvent compound, as detailed in Table 2. Thermochromic ternary reduction dyes generally comprise a chromophore, a chromophore activator, and an organic solvent. The chromophore (electron donor), such as spiropyran, bromoether, spiropyridine, or fluoride compounds, governs the system's color. Crystalline violet lactone (CVL) is widely used due to its vivid hue and high color-change sensitivity [24]. The chromophore activator (electron acceptor), including phenols, their derivatives, or Lewis acids, determines the depth of the system's color. The solvent acts as a medium linking the components and dictates the color-changing temperature of the reduction dye [25]. Typically, long-chain alkyl alcohols, carboxylic acids, or esters are employed, as they dissolve the donor and acceptor components effectively [26].

Table 2. Composition and Function of Organic Reversible TCMs.

Component	Classification	Function
Electron donor	Triarylmethane phthalides, fluorane, indole veratrole, spiropyrans, etc.	Determining color
Electron acceptors	Phenols, sulfonic acids, carboxylic acids, etc.	Determining color
Solvent compounds	Alcohols, esters, etc.	Determining color-change temperature

In general, the redox potential of the electron donor is close to that of the electron acceptor. When the temperature changes, electron transfer occurs between them, leading to structural changes in the donor molecule. As a result, the extent of electron transfer and color development varies with temperature, producing a reversible thermochromic response [27].

Hao et al. constructed a novel inorganic–organic hybrid material with electron donor–acceptor properties, exhibiting remarkable photochromic and thermochromic characteristics. The material, namely $[Hpyz]_2[Ag_2I_4]\cdot H_2O$ ($Hpyz^+$ = monoprotonated pyridine ion), shows diverse photochromic and thermochromic behaviors due to reversible hydration–dehydration processes, which induce intermolecular electron transfer and changes in charge-transfer states [28]. Pu et al. prepared a series of low-temperature reversible thermochromic dyes by dissolving CVL-based lactone compounds in methyl laurate at 7 °C [27].

3.2.3. Molecular Structural Changes

Certain TCMs exhibit extreme sensitivity to temperature variations at the molecular level, resulting in reversible thermochromic phenomena. Specifically, these phenomena arise from two main mechanisms: intermolecular proton transfer and changes in molecular structure. In the first mechanism, proton transfer occurs within molecules upon temperature elevation, altering the molecular structure and resulting in reversible thermochromic behavior. Schiff bases exemplify this pathway. In the second mechanism, molecular bond cleavage or distortion occurs at elevated temperatures, inducing molecular isomerization and producing reversible thermochromic effects.

3.2.4. Crystal Transformations

Crystal transformation is also an important thermochromic mechanism in some organic systems, although it is more commonly discussed in inorganic TCMs. The underlying processes may involve lattice contraction, lattice expansion, phase transition, or other changes in crystal packing, all of which can alter intermolecular interactions and optical behavior. Research indicates that increasing temperature strengthens the π–π interactions within 2,3-diphenylvinyl-5,6-dicyanopyrazine crystals, inducing lattice contraction and resulting in a color change [29]. At 174.5 °C, this compound undergoes a reversible transition from yellow to red. Liu et al. successfully prepared three TPENOMe-I-containing composites exhibiting reversible color changes by investigating the two-step isomerization process between the alcohol–ketone isomer and the cis- and cis-twisted ketone isomers, in combination with the compact crystal packing and polymorphism of TPENOMe-I [30].

3.2.5. Thermochromic Molecular Ring Opening

The color change in spiropyran and oxazine compounds is caused by C–O bond cleavage and the formation of conjugated systems upon temperature elevation. However, the high negative charge density of oxygen atoms in the naphthalene ring renders the structure unstable after ring-opening, resulting in limited color stability. Recently, inspired by trehalose molecules exhibiting remarkable multi-stimulus responsiveness and containing weak C_spiro–O bonds capable of isomerization under external stimuli, Han et al. designed and synthesized a novel, simple molecule (XG) by introducing a naphthalimide derivative. Initially, this molecule exhibited negligible photochromic, thermochromic, or mechanochromic properties. Following mild grinding, the compound displayed outstanding photochromic, thermochromic, and mechanochromic responses. During grinding, certain C_spiro–O bonds in the molecular structure are cleaved, inducing ring-opening isomerization and forming new C–O bonds [31]. Li et al. investigated the recovery of thermochromic liquid waste (TLW) generated during the development of CVL (crystal violet lactone)-type TCMs. By formulating a thermochromic liquid using a mixture of CVL, calcium chloride, n-octadecyl alcohol, and n-dodecyl alcohol, they found that C–O bonds are formed during the cooling process. Thermochromism can also be induced by benzene ring cleavage resulting from chemical bond breaking [32]. Moreover, color changes in organic materials are influenced by factors such as electronic spin states and pH values. For example, some studies have prepared transparent spin-crosslinked composite films that exhibit no color at 27 °C due to high-spin states; upon cooling, these films turn purple.

This color-changing system relies on acid–base indicators, including phenol red, phenolphthalein, and other weak acids (such as fatty acids), to provide protons. When heated to a specific temperature, the protons of the carboxyl groups become activated and react with substances exhibiting affinity, leading to proton gain or loss. Upon cooling, the protons in the carboxyl groups are restored, resulting in the recovery of the material's color.

3.3. Inorganic Reversible TCMs

Initial research on inorganic TCMs primarily focused on metals and metal halides, metal oxides, and polycrystalline materials composed of various metal oxides [33,34]. With advancing research, a growing variety of inorganic TCMs has been developed and studied, including vanadates, chromates, and tungstates, with metal ions originating from Group I–II elements or the IVB, VB, and VIB subgroups. Solid inorganic TCMs typically exhibit strong color stability, high-temperature resistance, good durability, and cost-effectiveness. However, these materials have certain limitations regarding color change uniformity, temperature response precision, and potential toxicity, which constrain their widespread practical application.

The color transformation in inorganic TCMs is mainly determined by lattice structure, electron transfer, ligand geometry, and changes in water of crystallization. Color shifts in inorganic oxides are generally associated with changes in their crystal structure, whereas those in inorganic complexes are related to modifications in coordination geometry or hydration level. Common inorganic TCMs and their color-changing principles are summarized in Table 3.

Table 3. Representative inorganic TCMs and their color-changing principles [23].

Inorganic TCMs	Color Change Mechanism
(1): VO, VO_2, V_nO_{2n-1}(n = 2–6, 8) Ti_2O_3, Ti_nO_{2n-1}(n = 3–6) NbO_2, Fe_3O_4, MnO_2, CuO	$XM + AO^+y + xe^- \leftrightarrow M_xAO_y$ (M = H, Li, Na; A = metal)
(2): Ag_2S, NiS	NR
(3): Ge-Te-Sb-S	Vitreous state → crystalline state transition
(4): Ge-S-Se, As-Se-(Ag, Cu)	Metal migration in amorphous structures
(5): $Cu_2[HgI_4]$ Red (T ≥ 69 °C) ↔ dark purple (T ≤ 6 °C) $Ag_2[HgI_4]$ Yellow (T ≥ 48 °C) ↔ red (T ≤ 5 °C)	Structure change

3.3.1. Crystal Transition

One mechanism for color change in inorganic reversible TCMs involves lattice displacement at specific temperatures. Specifically, the material's color shifts as it transforms from one crystalline form to another; when the temperature decreases, the lattice reverts to its original form, restoring the color [35]. Examples include Cu_2HgI_4 and Ag_2HgI_4, which exhibit a tetrahedral structure at low temperatures that transforms into a cubic structure upon heating. The temperature-dependent crystalline structures enable these compounds to undergo reversible color changes.

Cao et al. investigated four two-dimensional hybrid perovskite single crystals: $(HA)_2PbI_4$, $(BA)_2PbI_4$, $(PEA)_2PbI_4$, and $(NEA)_2PbI_4$. These crystals exhibited a color transition from orange to red during heating. In particular, the thermochromic effect in $(HA)_2PbI_4$ arises from a phase transition, whereas that in $(BA)_2PbI_4$, $(PEA)_2PbI_4$, and $(NEA)_2PbI_4$ is attributed to lattice expansion [36].

Nd_2MoO_6 exhibits reversible thermochromic behavior, changing from pale blue to green within the temperature range of 30–300 °C. Shifts in XRD peak positions indicate that the thermochromic effect of this material is directly related to lattice expansion at elevated temperatures, with the color change likely governed by lattice expansion and contraction processes [30].

3.3.2. Loss or Acquisition of Crystalline Water

The color change in inorganic TCMs is fundamentally attributable to alterations in coordination number. Most such substances are complexes of inorganic salts of cobalt and nickel containing water of crystallization. When heated to a specific temperature, the loss of crystalline water induces a color shift; upon cooling, these materials reabsorb water vapor from the environment, gradually restoring the original color [37]. For instance, iron phosphate dihydrate ($FePO_4 \cdot 2H_2O$) exhibits an orthorhombic or monoclinic structure. High-purity iron phosphate dihydrate appears as a white or pale yellow powder. As crystalline water is lost, the color progressively shifts to yellow, with the pure anhydrous compound presenting as a yellowish-white powder. Toupka et al. investigated a metal-doped molecular material—dihydrate [malonylester(1-)-κ^2O,O′] zinc(II) doped with iron—whose color-changing mechanism involves a shift in the Fe^{2+}/Fe^{3+} ion ratio

during dehydration upon heating, causing the material's color to transition from colorless to blue [38]. Furthermore, Halder et al. examined the reversible thermochromic properties and phase transitions of $MA_4PbI_6 \cdot 2H_2O$ perovskite driven by dehydration–rehydration processes [39].

3.3.3. Electron Transfer

Color changes in TCMs frequently arise from redox reactions induced by electron transfer. For example, hematite exhibits a reddish-brown hue resulting from two $2p(O^{2-}) \rightarrow 3d(Fe^{3+})$ charge transfers, a process whose color can be modulated by doping with other elements [40]. Similarly, $CrO_4{}^{2-}$ reacts with Pb^{2+} to form $PbCrO_4$. As the temperature increases, the enhanced oxidation capacity leads to greater Pb^{4+} generation, resulting in color intensification. Upon cooling, Pb^{4+} in $PbCrO_4$ is reduced back to Pb^{2+}, restoring the original color. $PbCrO_4$-type TCM coatings exhibit a color-change temperature of approximately 1000 °C, with a pronounced, reversible, and precise color-reversal process.

The thermochromic behavior of bismuth and its oxides follows a similar mechanism. $BiVO_4$ and its derivatives exhibit reversible thermochromic transitions from bright yellow to deep orange. Bi_2O_3 and its derivatives show a gradual increase in isotropic lattice parameters during heating; at the phase transition temperature (β phase to δ phase), the color changes abruptly. $Bi_2Mo_3O_{12}$ undergoes a transition from milky white to bright yellow. The thermochromic mechanisms of these materials are all based on thermally induced charge transfer between oxygen and bismuth atoms. The recently developed $\beta - Bi_2Sn_2O_7$ is a continuously reversible thermochromic material, exhibiting a color change from pale yellow to reddish brown [41].

3.3.4. Ligand Geometric Changes

Reversible alterations in ligand geometry within materials upon temperature changes induce color shifts. For example, $[(C_2H_5)_2NH_2]_2CuCl_4$ exhibits a color transition temperature of 43 °C, reversibly shifting between green and yellow hues, primarily due to structural changes or variations in ligand number. These reversible TCMs demonstrate stable color-changing properties, excellent thermal stability, and pronounced color differences.

Similarly, the thermochromic behavior of Cr^{3+} arises from the expansion of its ionic lattice upon heating. In compounds containing octahedrally coordinated Cr^{3+} ions, the interionic distances between Cr^{3+} centers change with temperature, inducing corresponding color shifts in the compound [42]. Moreover, Cu-Me-DPSO has been shown to emit yellow or orange luminescence at different temperatures, with its morphological changes attributed to alterations in coordination geometry within the excited state [43].

3.4. Other TCMs

Beyond inorganic and organic TCMs, certain structural materials with engineered properties unattainable in natural counterparts have been developed, typically classified as engineered composites. In addition, non-dye-based TCMs represent another extensively researched domain, encompassing quantum dots, plasmonic structures, photonic crystals, conjugated polymers, Schiff bases, and liquid crystals [44].

The properties of these materials do not arise from traditional dyeing compounds themselves, but instead stem from unique functionalities unattainable by conventional materials. Common advanced material substrates include biomimetic plastics, thermoelectric materials, aerogels, and light-manipulating materials.

Recent research has centered on two primary categories of such beyond-material systems. The first category comprises materials exhibiting color-changing mechanisms associated with distinct nanoscale effects, including quantum dots, plasmonic structures,

and photonic crystals. The second category encompasses non-dye-based TCMs, such as conjugated polymers, liquid crystals, and Schiff bases [45].

3.4.1. Quantum Dots

Quantum dots (QDs) are nanoscale luminescent particles composed of inorganic semiconductors from Groups II–VI (e.g., CdSe and CdTe) or III–V (e.g., InP), typically measuring 2–10 nm in size. They exhibit unique optical properties that are distinct from those of the bulk materials. QDs can absorb incident light at one wavelength and emit light at a different wavelength [45]. In the built environment, quantum dots hold potential for mitigating urban overheating through mechanisms such as fluorescent cooling and temperature-responsive photoluminescence. One potential application involves blending QDs with polymethyl methacrylate and other polymers exhibiting good adhesion to conventional building substrates, which can then be coated onto building surfaces [46].

3.4.2. Plasmonics

Plasmonic phenomena arise when electrons in conductive materials are delocalized and can move freely, influencing the optical properties of nanoparticles. The wavelength of surface plasmon resonance (SPR) can be tuned by adjusting multiple factors, including nanoparticle size, shape, and spacing [47,48]. In recent studies, plasmonic materials such as gold nanorods have been incorporated into photothermal-chromic smart windows. These windows consist of polyvinyl alcohol (PVA) and thermochromic dyes. The transition temperature of the dyes can be enhanced by heating [49]. Furthermore, plasmonic technology finds extensive application in enhancing the efficiency of photovoltaic devices.

3.4.3. Photonic Crystals

A photonic crystal consists of a series of discrete parallel planes, known as Bragg planes. When light enters the photonic crystal, part of it is reflected at the first plane, while the remainder passes through to the second plane. According to Bragg's law, if the path difference between the two waves equals an integer multiple of the wavelength, they undergo constructive interference, resulting in a pronounced reflected peak [50]. When responsive polymeric materials are incorporated into photonic crystal structures, the materials exhibit distinct structural color changes in response to external stimuli, offering significant potential for applications in anti-counterfeiting technology and smart sensors [51]. Moreover, by customizing the surface microstructures of photonic crystals, these structural color materials demonstrate angle invariance, enabling broad applications in decoration, coatings, painting, and display devices [50].

3.4.4. Conjugated Polymers

Conjugated polymers constitute a class of organic polymers exhibiting semiconductor properties, characterized by alternating single and double bonds along their backbone and the presence of delocalized electrons. Thermochromic conjugated polymers are primarily classified into four types: polyacetylenes, polydiacetylenes (PDA), polythiophenes, and poly(phenylene vinylidenes). Their thermochromic behavior arises from the shortening of the effective conjugation length [45]. For example, polydiacetylene (PDA) films embedded in polyvinyl alcohol (PVA) undergo color transitions from blue to red. Carotenuto et al. successfully synthesized reversible thermochromic nanocomposites based on thiol-capped silver nanoparticles via chemical precipitation, exhibiting remarkable thermochromic properties [47].

3.4.5. Schiff Bases

Schiff bases constitute a class of smart materials whose optical properties can be readily manipulated by environmental stimuli such as light, heat, or electric current. Upon temperature elevation, protons within the Schiff base molecule undergo proton transfer, altering the molecular structure and thereby exhibiting reversible thermochromic behavior. This proton-transfer mechanism fundamentally underlies the color-changing properties of Schiff base compounds.

Schiff bases can be categorized into two types: organic Schiff bases and organometallic Schiff bases. For example, salicylaldehyde acetamide, an organic Schiff base containing an –OH group, can form intramolecular hydrogen bonds. Upon heating, protons rapidly transfer from the oxygen atom to the nitrogen atom, causing a tautomeric shift from the ketone to the cis-ketone form, resulting in a reversible color change.

Organometallic Schiff bases also exhibit color changes upon heating. The thermochromic properties of Schiff base metal complexes arise from alterations in ligand field strength and coordination geometry. For instance, the reversible continuous thermochromism of copper complexes is attributed to changes in ligand field strength and symmetry [52].

3.4.6. Origami Structures

Origami structures constitute responsive thin-film architectures in which the material is divided into periodically arranged crystalline units. These units can bend or invert in response to external stimuli, thereby modulating solar energy absorption and reflection. This approach introduces geometric defects or incorporates thermoresponsive materials at specific locations within each unit cell to achieve controlled deformation orientations.

3.4.7. Liquid Crystals

As a reversible thermochromic material, liquid crystals selectively absorb certain wavelengths of white light while reflecting polarized light of specific wavelengths. This enables the surface to simultaneously reflect and transmit light of two distinct colors, with the hue shifting as the helical structure elongates or contracts in response to temperature. The helical structure exhibits high sensitivity to thermal variations, altering its extent of twist accordingly.

Reversible liquid crystal TCMs are primarily composed of cholesteric liquid crystals. The cholesteric phase is a type of nematic phase exhibiting a helical arrangement rather than linear alignment. The most critical parameter controlling the optical properties and color of the cholesteric phase is the pitch, defined as the vertical distance required to complete one full helical rotation. The pitch is influenced by factors such as temperature, electric fields, magnetic fields, and chemical environment.

Figure 1 illustrates helical structures of cholesteric liquid crystals. As shown in Figure 1, the helical structure exhibits pitch variation with temperature, altering the wavelengths of reflected visible light and thereby inducing color changes. Because the pitch length corresponds to visible light wavelengths, these TCMs possess distinctive optical properties and pronounced thermochromic characteristics.

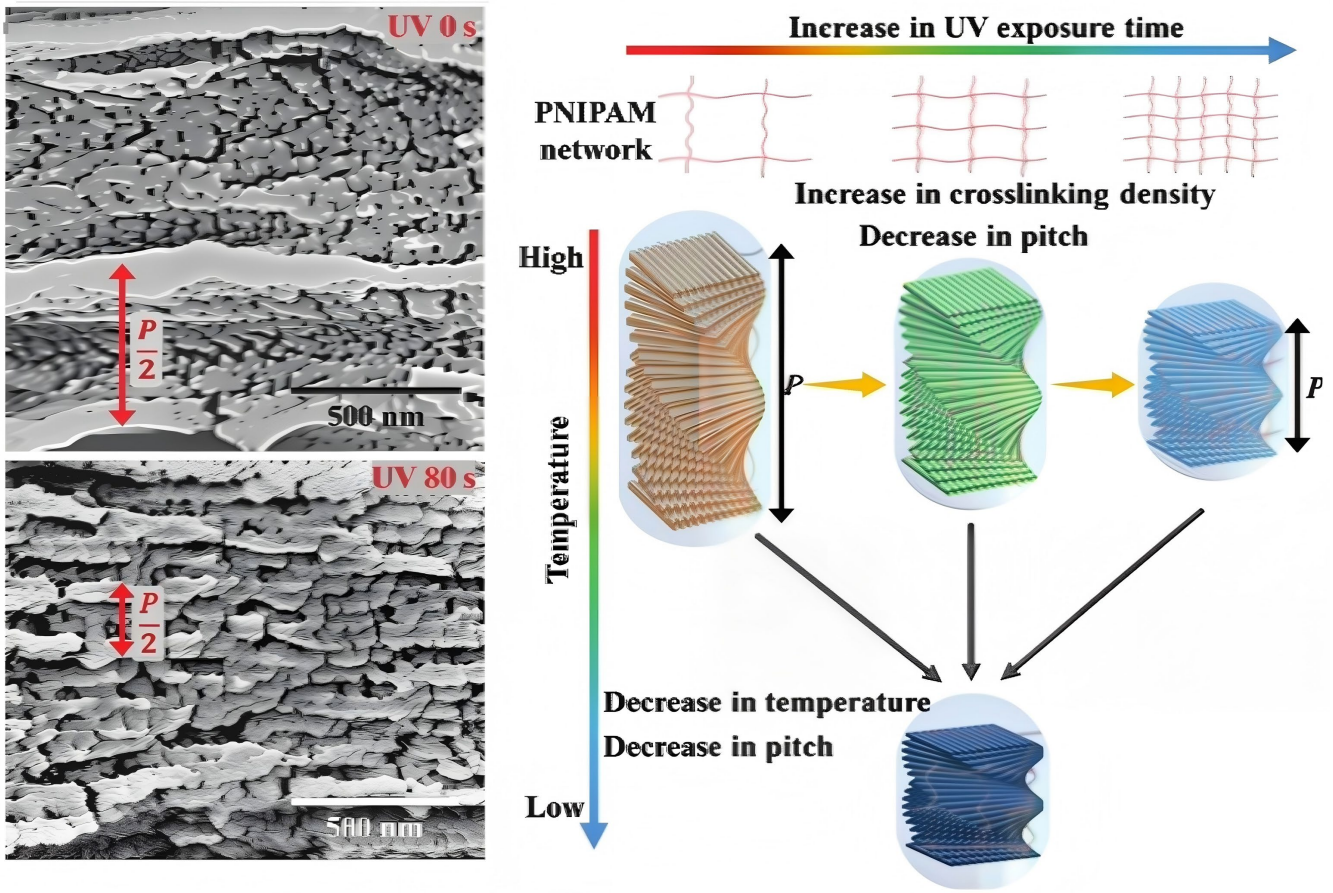


Figure 1. Cholesteric liquid crystal's helical structure. Reproduced from Ref. [53].

Liquid crystals have found extensive applications across multiple fields, including temperature sensors, photovoltaics, and smart windows. In temperature sensors, liquid crystals indicate temperature through reversible color changes. M. Turvey et al. investigated ultrasonic displacement induced by localized absorption in thermochromic liquid crystals. These materials are also employed in smart windows, where they regulate solar incidence by adjusting solar reflectance in response to temperature or electric fields [54].

Overall, TCMs may outperform many conventional passive materials in mitigating urban overheating because their optical properties change with temperature. This adaptive response can help reduce annual energy demand [45]. The following section discusses several emerging non-dye thermochromic systems. The performance of conventional non-dye TCMs is largely constrained by natural limitations, whereas nanoscale TCMs offer the unique advantage of precise control over their optical properties through fine-tuning multiple parameters. These characteristics make them a promising frontier in research on TCMs.

4. Preparation Methods for TCMs

TCMs are commonly prepared through three main routes: solid-state synthesis, liquid-phase methods, and vapor-phase deposition. These routes are suitable for different material forms and application scenarios. In general, solid-state methods are mostly used for bulk powders and phosphors, liquid-phase methods are more suitable for nanoparticles and solution-processed coatings, and vapor-phase deposition is preferred for dense functional films, particularly VO_2-based coatings for smart-window applications. Readers interested in more detailed process descriptions may refer to Refs. [55–57].

4.1. Solid-Phase Methods

The solid-state method is still widely used for preparing inorganic thermochromic powders and phosphors because it is simple, inexpensive, and suitable for large-scale production. Its main disadvantages are high energy consumption, relatively poor control over particle size, and the possible introduction of impurities [58]. In essence, the process involves diffusion, reaction, nucleation, and crystal growth; when nucleation dominates over growth, smaller particles are more likely to form.

This route has been used for a range of thermochromic systems, including crystal-violet/boric-acid composites and $La_{1-x}Sr_xMnO_3$ compounds [59]. It has also been applied to Nd_2MoO_6, which shows a reversible color change from light blue to green between 30 and 300 °C [60], and to several thermochromic phosphors such as CMO:Pr^{3+}, Pr^{3+}-doped $Mg_3Gd_2Ge_3O_{12}$, and $KGaSiO_4$:Eu^{3+}, where composition tuning was found to influence color response and application potential in sensing or anti-counterfeiting [40,61,62]. Overall, the solid-state route remains practical for conventional phosphor-based and oxide TCMs, although it is less suitable when precise control of microstructure is required.

4.2. Liquid-Phase Deposition Methods

Liquid-phase methods mainly include sol–gel, hydrothermal, and chemical precipitation techniques [63]. These methods are attractive because they provide better control over composition, particle size, and morphology through adjustments in precursor concentration, temperature, pH, stirring conditions, and reaction time. They are widely used for oxides, composite oxides, and ultrafine metallic powders.

4.2.1. Sol–Gel Method

The sol–gel method is one of the most widely used laboratory-scale routes for preparing nanostructured TCMs. Compared with gas-phase deposition, it requires simpler equipment and is more flexible for composition tuning and morphology control. In a typical process, metal alkoxides, metal salts, or molecular precursors are dissolved to form a sol, followed by gelation and annealing to obtain the target crystalline phase [2].

For VO_2-based materials, sol–gel processing has been widely used to tailor optical performance and transition behavior. Representative studies include the optimization of annealing conditions for VO_2 formation [64], the deposition of nanoporous SiO_2 on VO_2 films to improve transmittance [65], and the preparation of pure and W-doped VO_2 films [51]. The same route has also been extended to W/Si-modified VO_2 gels [66,67], nanoscale VO_2 particle films [68], TiO_2@W-VO_2 co-doped films [69], and high-purity VO_2 films derived from V_2O_5 precursors [70,71]. Taken together, these studies show that the sol–gel method is especially useful when compositional flexibility and low-cost processing are more important than deposition speed or industrial throughput.

4.2.2. Hydrothermal Method

The hydrothermal method is a soft-chemical route carried out in a sealed high-temperature, high-pressure environment, where poorly soluble precursors can dissolve and recrystallize under controlled conditions [72,73]. It has been widely used for the synthesis of single crystals, ceramic powders, and nanostructured oxides, and it is particularly valuable for preparing VO_2 nanoparticles and doped nanostructures with controlled phase composition.

In thermochromic research, hydrothermal synthesis has played an important role in reducing the phase-transition temperature and tailoring particle morphology. Early work showed that W-containing systems could promote the formation of rutile VO_2 and reduce the transition temperature to around room temperature [74]. Subsequent studies reported

Mo-doped VO_2 [75,76], VO_2(M)/SnO_2 heterostructure nanorods [76], solvothermally prepared copper(I) thiol coordination polymers with chromic behavior [43], machine-learning-guided hydrothermal synthesis of VO_2 nanoparticles [77], rare-earth/W co-doped VO_2 nanoparticles [78], and boron-doped VO_2 powders with composition-dependent transition temperatures [79]. Microwave-assisted hydrothermal synthesis has also been shown to shorten reaction time while maintaining product quality [80]. Overall, the hydrothermal route is especially suitable for preparing VO_2(M) nanostructures with tunable transition behavior through precursor and parameter design [81].

4.3. Vapor-Phase Deposition Methods

Vapor-phase deposition is mainly used for thin-film fabrication and can be divided into chemical vapor deposition (CVD) and physical vapor deposition (PVD). Compared with powder-based or solution-based methods, vapor-phase routes are more suitable for applications requiring dense, uniform, and highly controlled films.

4.3.1. Chemical Vapor Deposition

CVD is one of the most established methods for preparing high-quality functional thin films and has long been used for VO_2 deposition [82–84]. It is particularly useful when film crystallinity, uniformity, and large-area deposition are important. The main challenges in VO_2 applications, including high transition temperature, undesirable coloration, and limited thermochromic efficiency, have motivated extensive work on doped and multilayer films prepared by CVD [85].

Current CVD-based approaches include APCVD, AACVD, electric field-assisted CVD, and Mist-CVD. Representative studies include gradient TiO_2/VO_2 films prepared by APCVD [86], hybrid CVD strategies for TCM fabrication [55–57], CeO_2- or TiO_2-modified VO_2 films obtained by AA/APCVD [55], VO_2 films deposited from vanadium acetylacetonate precursor systems on coated glass substrates [56,57], and low-cost Mist-CVD preparation of VO_2 thin films [87]. N-doped VO_2 films grown on synthetic mica have also been reported, with transition temperatures close to 30 °C [88]. Beyond VO_2, CVD has been used for halide-hybrid perovskite films [89], TiO_2/VO_2 multilayers [90], region-selective VO_2 growth using SiO_2 masks [91], and the preparation of reversible thermochromic $Sn_2P_2S_6$ films with building-energy relevance [92]. In short, CVD remains one of the most important routes for application-oriented thermochromic films, especially when precise film engineering is needed.

4.3.2. Physical Vapor Deposition

PVD is also widely used for thermochromic thin films because it offers relatively low processing temperatures, good environmental compatibility, and broad substrate adaptability [84,86]. Among PVD techniques, reactive sputtering is the most common route for VO_2, including DC sputtering, RF sputtering, and magnetron sputtering [93,94].

A large number of VO_2-based films have been prepared by sputtering-related methods. These include DC reactive magnetron sputtering [53,95], low-temperature RF sputtering of W-doped VO_2 nanoparticles onto glass [96], Ga-implanted VO_2 films [97], and Mo-doped VO_2 films produced through magnetron sputtering combined with post-oxidation annealing [98]. Simplified DC magnetron sputtering routes have also been proposed for films of different thickness ranges [99]. In multilayer and composite systems, RF magnetron sputtering has been used to fabricate ZnO/VO_2-based structures with improved crystallinity and optical performance [100], while pulsed laser deposition has enabled V/CZ/V composite films containing Cu-Zr alloy nanoparticles [101]. Overall, PVD is especially useful for high-quality VO_2 films and multilayer architectures where thickness, interface structure, and optical performance must be carefully controlled.

4.4. Other Preparation Methods for TCMs

In addition to the major preparation routes described above, some studies have explored electrochemical methods and polymer-assisted deposition (PAD), mainly for specialized substrates or specific film architectures.

4.4.1. Electrochemical Method

Electrochemical deposition is attractive because it is simple, inexpensive, and suitable for substrates with complex geometries. However, early reports showed that the resulting VO_2 layers could be very thin and require long post-treatment times [102]. Improved electrodeposition routes have since been developed to obtain thicker VO_2 films on conductive substrates [103]. This method has also been extended to multifunctional thermochromic systems, such as rhodium(I) isocyanide-based ionic liquids with thermochromic, fluorescent, and chemo-chromic behavior [104], chlorine-nickel(II) solutions with thermochromic properties, and VO_2(B) films formed on carbon cloth through electrodeposition followed by thermal annealing [105]. Although less widely used than sputtering or sol–gel processing, electrochemical methods remain useful when low cost and substrate compatibility are priorities.

4.4.2. Polymer-Assisted Deposition Method

PAD is a chemical solution deposition technique in which polymer chains coordinate metal ions and help distribute them uniformly, making it possible to form homogeneous metal oxide films at relatively low cost [106]. For TCMs, this approach has mainly been applied to VO_2-based films. Titanium-doped VO_2 prepared by PAD has shown strong near-infrared modulation, with transmittance changes approaching 50% at 2000 nm [107]. PAD has also been used to prepare VO_2 films on Al_2O_3 substrates with periodic grating-like surface structures [108], as well as VO_2 films on mica substrates followed by rapid annealing under different conditions [109]. Compared with conventional solution routes, PAD offers a useful alternative when uniform ion distribution and controlled polycrystalline film growth are required.

5. Performance Testing Methods for TCMs

Performance testing is essential for judging whether TCMs are suitable for practical use. In most studies, the key concerns are straightforward: how obvious the color change is, how fast it occurs, whether it is reversible, and whether the material remains stable under repeated use or environmental exposure. For this reason, the evaluation of TCMs usually combines colorimetric analysis, spectral analysis, and complementary tests related to response rate, durability, mechanical reliability, and structural evolution. Together, these measurements help connect visible color change with the underlying thermal and structural processes, and they also provide the basis for applications in building energy saving, information display, smart textiles, and thermal-management systems.

5.1. Colorimetric Analysis

Colorimetric analysis is one of the most direct ways to evaluate the visible response of TCMs. It is mainly used to describe hue, lightness, and color difference at different temperatures, and therefore to identify the effective color-change interval and the intensity of the visual response. In addition to research use, this method is also useful for quality control because it allows comparison of color performance across samples or batches.

In practice, color is commonly measured with a spectrophotometer or colorimeter under controlled illumination and observation conditions. The most widely used system is the CIELAB color space, which represents the sample by the parameters ΔL^*, Δa^*, and

Δb*, as shown in Table 4 [110]. The overall color difference between two states is usually expressed by ΔE*, which is calculated as:

$$\Delta E* = \sqrt{\Delta L*^2 + \Delta a*^2 + \Delta b*^2} \quad (1)$$

where ΔL*, Δa*, and Δb* denote the respective differences in luminance and chromaticity coordinates between the two states.

Table 4. Chromaticity Parameters.

Parameter	Parameter Characterization	Value	Meaning
ΔL*	Luminance	>0	Becomes brighter
		<0	Darker
Δa*	Red–green axis	>0	Red
		<0	Green
Δb*	Yellow–blue axis	>0	Yellow
		<0	Blue

Representative studies show how this method is used to compare thermochromic sensitivity and optimize composition. For example, Guo et al. [111] used colorimetric analysis to evaluate $ZnWO_4$-based systems and showed that transition-metal doping significantly enhanced thermochromic response. Ma et al. [112] applied thermochromic and energy-storage microcapsules to polyester/cotton blend fabric through a waterborne polyurethane coating process, and assessed the thermochromic behavior of the coated fabric by combining color change observation with color-property analysis. Li [113] used the same approach to optimize the core-to-shell ratio of thermochromic microcapsules, while Wang [114] combined color observation with UV-Vis analysis to confirm the reversible photothermal color change in TC-micro PCMs. Taken together, these studies show that colorimetric analysis is particularly useful for comparing color intensity, transition range, and formulation effects in a simple and quantitative way.

5.2. Spectral Analysis

Spectral analysis provides a more detailed view of thermochromic behavior by measuring how absorption, reflection, or transmission changes with temperature. Compared with colorimetric analysis, it offers more complete wavelength-dependent information and is especially important when the intended application depends on optical regulation in specific spectral regions, such as the visible or near-infrared range.

For coatings, films, and glazing materials, spectral transmittance T(λ) or reflectance r(λ) is usually measured with a spectrophotometer, and integrated optical parameters are then obtained using standard weighting spectra. In smart-window studies, the luminous transmittance ($T_{_lum}$) is commonly defined over the visible range (380–780 nm) as

$$T_{lum} = \frac{\int_{380}^{780} D_{65}(\lambda)V(\lambda)T(\lambda)d\lambda}{\int_{380}^{780} D_{65}(\lambda)V(\lambda)d\lambda} \times 100\% \quad (2)$$

where D65(λ) is the relative spectral power distribution of the standard daylight illuminant and V(λ) is the photopic luminous-efficiency function. The solar transmittance ($T_{_sol}$) is commonly defined over 300–2500 nm as:

$$T_{sol} = \frac{\int_{300}^{2500} S_\lambda T(\lambda)d\lambda}{\int_{300}^{2500} S_\lambda d\lambda} \times 100\% \quad (3)$$

where $S_{_\lambda}$ is the solar spectral irradiance, commonly taken from ASTM G173 [115,116]. The solar modulation ability is then expressed as $\Delta T_{_sol} = T_{_sol,cold} - T_{_sol,hot}$. Using the same solar weighting spectrum, the solar reflectance (SR) can be written as

$$SR = \frac{\int_{300}^{2500} S_\lambda r(\lambda) d\lambda}{\int_{300}^{2500} S_\lambda d\lambda} \times 100\% \quad (4)$$

and the reflectance difference between two thermochromic states is $\Delta SR = SR_{_cold} - SR_{_hot}$. For clarity and consistency, the optical response discussed in this review is divided into the ultraviolet (300–380 nm), visible (380–780 nm), and near-infrared (780–2500 nm) regions [110,117]. In practical evaluation, larger values of $\Delta T_{_sol}$ or ΔSR generally indicate stronger solar regulation and therefore greater potential for building energy-saving applications.

Typical examples include the work of Wang et al. [118], who studied VO_2(M) nanosheet composite films with different thicknesses and found strong modulation in the near- to mid-infrared region, especially between 1900 and 3500 nm. Zhang et al. [119] used UV-Vis spectroscopy to track the effect of Mn doping on $Zn_{1-x}Mn_xO$ and showed that increased visible absorption was closely associated with the observed macroscopic color deepening. These studies illustrate that spectral analysis is indispensable when the material is intended not only to change color, but also to regulate heat or radiation.

5.3. Other Performance Testing Methods for TCMs

Colorimetric and spectral measurements are often not enough on their own. For practical applications, TCMs also need to be evaluated in terms of response time, cyclic stability, reversibility, mechanical reliability, and microscopic mechanism. These tests are usually selected according to the application scenario.

(1) Thermal response time (τ)

Thermal response time describes how quickly a material reaches a stable color-changing state after heating or cooling. It is an important indicator for applications that require fast or near-real-time optical regulation. The response depends on factors such as thermal conductivity, thickness, morphology, dispersion of active components, and interfacial thermal resistance [120]. It can be estimated from time-dependent absorbance changes using:

$$\tau = \frac{t_2 - t_1}{\ln(A_2/A_1)} \quad (5)$$

where t_1 and t_2 denote the times required for the absorbance to reach state 1 and state 2, respectively, and A_1 and A_2 represent the corresponding absorbance values.

Liu et al. [121] used this approach to evaluate a PNIPAm gel system and found that the sample became turbid and stabilized within about 20 s at 40 °C, indicating a rapid thermal response.

(2) Durability and stability

Durability testing is used to determine whether thermochromic behavior can be maintained after repeated cycling or long-term environmental exposure. Common approaches include heating-cooling cycles, UV irradiation, and combined heat–humidity aging. Yan et al. [122], for example, performed 20 color-change cycles on OTM-GO/Al_2O_3/PDMS nanocomposites and found that the spectral curves remained nearly unchanged, indicating good long-term stability.

Color retention can also be quantified through the color retention ratio (CRR):

$$CRR = \frac{A - B}{A} \times 100 \quad (6)$$

where A is the initial absorbance at a given temperature and B is the absorbance after a certain number of cycles under the same conditions. A higher CRR indicates better resistance to fading.

(3) Color shift temperature range (ΔT)

The color-shift temperature range reflects the temperature interval over which obvious color change occurs:

$$\Delta T = T_c - T_d \quad (7)$$

where T_c is the upper limit of the thermochromic material's color-change temperature, and T_d is the lower limit. A narrower ΔT facilitates a sharp color transition, whereas a wider ΔT is more suitable for applications requiring gradual temperature regulation.

For example, Zhou et al. [123] subjected ILDHs/TESM to 100 heating–cooling cycles and found that the change in ΔE_RT before and after cycling was only 0.58 NBS, well below the threshold of obvious human perception, which indicates excellent color stability. Zhang et al. [124] further examined the photostability of red fluorophore dyes and showed that their absorbance decreased only slightly after irradiation, suggesting that these compounds are suitable as chromic components in thermochromic systems.

(4) Reversibility (γ)

Reversibility is critical for materials that must undergo repeated heating–cooling cycles without losing their thermochromic function. It is usually assessed by tracking changes in color parameters, absorbance, or transmittance over repeated cycles [34,120].

Zhu et al. [125] evaluated inorganic VO_2-based thermochromic films over multiple heating-cooling cycles and found that the optical response and color remained highly stable from cycle to cycle, exhibiting excellent reversible durability.

(5) Mechanical Properties

Mechanical testing becomes especially important when TCMs are used in coatings, fibers, or composite phase-change systems. Tensile, flexural, and fatigue tests are commonly used to judge whether the material can maintain its integrity during repeated thermal cycling.

For instance, Zhao et al. [126] compared HPCMs and Micro-HPCMs and found that the addition of thermochromic microcapsules could improve tensile strength and stiffness, showing that mechanical performance should be considered together with color behavior for practical design.

(6) Analysis of color-changing mechanism

Understanding the mechanism of thermochromism is important not only for explaining observed behavior but also for guiding material design. In reversible systems, the main mechanisms usually include crystal-structure phase transition, crystal-field variation, bandgap change, temperature-dependent ligand rearrangement, and defect regulation. Typical examples include VO_2 [127], Cu_2HgI_4 [128], Cr^{3+}-doped Al_2O_3 [129], CuO quantum dots [130], $(Et_2NH_2)_2CuCl_4$ [131], and $Zn_{1-x}Co_xO$ [132]. By contrast, irreversible thermochromic behavior is often associated with decomposition, oxidation, dehydration, or high-temperature solid-state reactions [111].

Because these microscopic processes cannot be identified from color data alone, thermochromic studies usually combine several structural and thermal characterization meth-

ods. XRD is commonly used to track temperature-dependent phase evolution [133], SEM is used to examine morphology changes during heating and cooling [134], and DSC is used to identify phase-transition or melting-related thermal events [135]. For example, recent studies on reversible thermochromic nanofiber membranes used differential scanning calorimetry (DSC) to confirm that the macroscopic color-change phenomenon is strictly governed by the melting and crystallizing processes of the encapsulated phase-change components [136].

5.4. Typical Application Cases

In practical research, thermochromic performance is rarely evaluated by a single test. Most studies combine colorimetric, spectral, thermal, and structural methods so that visible response, thermal behavior, and long-term stability can be assessed together.

Li et al. [137] used this kind of integrated strategy to study thermochromic energy-storage materials based on crystal violet lactone, cresyl red, and octadecyl alcohol. Their evaluation included color observation, ΔE analysis, transition-temperature determination, DSC, FTIR, thermal stability, and cycling performance, which together provided a clear picture of both thermochromic behavior and energy-storage function. Kumar et al. [138] adopted a similar multi-technique approach for inorganic thermochromic coatings, combining temperature-dependent UV-Vis spectroscopy, X-ray diffraction (XRD), and morphological analysis to link structural lattice expansion with optical response. For building-related applications, Long et al. [139] further proposed the concepts of Energy Saving Equivalent (ESE) and Energy Saving Index (ESI), which connect the optical response of VO_2 glass with building energy-consumption models and therefore provide a more application-oriented basis for material evaluation.

The performance of TCMs should not be evaluated solely by whether they change color. Depending on the intended application, the key criteria may also include transition temperature range, color intensity, response speed, reversibility, stability, mechanical reliability, and application-specific metrics such as ΔSR, ESE, or ESI. The combined use of colorimetric, spectral, thermal, and structural methods not only improves the reliability of performance evaluation, but also helps clarify how macroscopic color change is linked to microscopic material behavior.

6. Performance Enhancement of TCMs

TCMs (such as VO_2) have attracted considerable attention due to their significant energy-saving potential in applications like smart windows and energy-efficient buildings. However, conventional VO_2 materials still exhibit several inherent limitations, including a relatively high phase-change temperature (approximately 68 °C), a yellowish coloration, insufficient visible light transmittance, and limited solar modulation efficiency. These factors together limit their large-scale application. To address these bottlenecks, recent studies have focused on structural design, process optimization, and the development of more environmentally friendly thermochromic systems.

6.1. Structural Design Optimization Strategies

Through rational structural design, it is possible to achieve simultaneous tuning of optical properties, phase transition temperature, and environmental stability, without altering the fundamental crystal structure of VO_2. Typical strategies include core–shell, hybrid/composite, and multilayer structures, as well as nanostructure designs.

6.1.1. Core–Shell Structures

The core–shell structure forms a “core–interface–shell” gradient architecture at the microscale by coating VO_2 particles with one or more functional shells. On the one hand, the

shell layer acts as a physical barrier, inhibiting direct contact between VO_2 and atmospheric oxygen and moisture, thereby enhancing the material's chemical and environmental stability. On the other hand, dielectric or polymer shells can modulate the interfacial refractive index and scattering behavior, effectively improving the visible light transmittance and color appearance of films or coatings.

It should be noted, however, that preparing core–shell structures typically requires precise control over particle size, shell thickness, and composition, involving relatively complex processes and potentially higher costs. In specific studies, various VO_2-based core–shell structures have been engineered to enhance thermochromic performance. For instance, the solar modulation efficiency (ΔT_{sol}) of VO_2/Al-O core–shell structures reached 9.62% [140]. SiO_2/VO_2 core–shell structures achieved 7.5% ΔT_{sol} at a visible light transmittance (T_{lum}) of 55.3%, with a phase transition temperature (T_τ) of 55.7 °C [141]. VO_2@TiO_2 nanorod structures exhibited a ΔT_{sol} of 15.35% at T_{lum} = 27.4%, with T_τ = 62.4 °C [142]. VO_2@ZnO core–shell nanoparticles exhibited a ΔT_{sol} of 19.1% at T_{lum} = 51.0%, with T_τ = 63.6 °C [143].

Polymer shells have also demonstrated favorable modulation effects. For instance, VO_2@PMMA-b-PHFBMA core–shell nanoparticles significantly reduced the phase transition temperature to T_τ = 54.46 °C [144], while VO_2(M)@CeO_2 core–shell nanospheres exhibited T_τ = 40.6 °C [145]. VO_2(M)@SnO_2 core–shell nanoparticles achieved an outstanding solar modulation efficiency of 25.0% at T_{lum} = 35.0% [146]. Moreover, W-doped VO_2@AA core–shell nanoparticles attained a ΔT_{sol} of 10.18% at T_{lum} = 70.52%, further lowering the phase transition temperature to 34.53 °C [147], as detailed in Table 5.

Table 5. Thermochromic performance of VO_2 based on core–shell structure strategy.

Category	Material/Structure	T_{lum} (%)	ΔT_{sol} (%)	T_τ (°C)	References
Core–shell Structure	VO_2/Al-O core–shell structure	NR	9.62	NR	[140]
	SiO_2/VO_2 core–shell structure	55.3	7.5	55.7	[141]
	VO_2@TiO_2 core–shell nanorods	27.4	15.35	62.4	[142]
	VO_2 @ PMMA-b -PHFBMA core–shell nanoparticles	NR	NR	54.46	[144]
	VO_2@ZnO core–shell nanoparticles	51.0	19.1	63.6	[143]
	VO_2(M)@CeO_2 core–shell nanospheres	NR	NR	40.6	[145]
	VO_2(M)@SnO_2 core–shell nanoparticles Particles	35.0	25.0	NR	[146]
	W-VO_2@AA core–shell nanoparticles	70.52	10.18	34.53	[147]

These results demonstrate that, through judicious selection of shell materials and structural parameters, core–shell structures offer significant advantages in regulating the optical properties, phase-change temperature, and environmental durability of VO_2, providing a crucial pathway toward high-performance thermochromic smart windows.

To improve cross-study comparability, the following tables summarize not only the reported optical performance metrics, but also the main experimental context wherever available from the original references, including film thickness or characteristic size, substrate, the calculation/integration method used for the reported optical parameters, the definition of switching temperature, hysteresis width, and key measurement conditions such as geometry and spectral range.

6.1.2. Hybrid Structures

Hybrid structures typically achieve synergistic physical and chemical properties by combining TCMs with other inorganic or organic functional components at the microscale. For instance, hybridizing inorganic VO_2 with organic TCMs or polymer matrices simultaneously harnesses VO_2's reversible metal–insulator phase transition behavior and the

organic components' advantages in flexibility, processability, or color regulation. This strategy expands the applications of such materials in smart windows, flexible devices, and sensing technologies [148]. However, disparities in thermal expansion coefficients, interfacial bonding, and compatibility between different components pose challenges for structural design and process implementation. Consequently, meticulous optimization in material selection and interface engineering is required.

Broadly speaking, performance enhancement strategies based on hybrid structures primarily encompass two categories: elemental doping and multiphase composites. Elemental doping alters the carrier concentration and lattice constant of VO_2 at the lattice level, thereby regulating phase transition temperatures and optical responses. In addition, multiphase composites and bilayer/multilayer structures optimize $T_{_lum}$ and $\Delta T_{_sol}$ through interfacial effects and optical interference phenomena.

Regarding single-element doping, Si, Zr, and Mg significantly enhance the $T_{_lum}$ of VO_2 films to 54.7–61.4%, while retaining approximately 10% solar modulation capability ($\Delta T_{_sol}$) [149–151]. Notably, W-doped VO_2 coatings demonstrate exceptional performance, lowering the phase transition temperature ($T_{_\tau}$) to approximately 22 °C [152]. H-doped systems can achieve $T_{_\tau}$ around 30.0 °C [153].

Building upon this, co-doping strategies (such as W/Zr, W/Mg, Hf/W, etc.) [154–156] seek to achieve a more favorable balance between high transmittance, relatively high modulation capacity, and low phase transition temperature. For instance, the W/Zr co-doped system achieves a $T_{_lum}$ of 60.7% while maintaining a $\Delta T_{_sol}$ of 10.6%. Similarly, the SiO_2/W co-doped system yields a $T_{_lum}$ of approximately 48.5% [157].

Furthermore, constructing bilayer structures by combining VO_2 with other media or functional layers proves effective in enhancing overall performance. VO_2/TiO_2 bilayer films exhibit outstanding integrated properties with $T_{_lum}$ = 61.5% and $\Delta T_{_sol}$ = 15.1% [158], while Si–Al/VO_2 bilayer coatings further elevate $\Delta T_{_sol}$ to 18.9% [159]. These studies demonstrate that elemental doping and multiphase hybridization designs can effectively mitigate the inherent trade-off between light transmittance, modulation capability, and phase transition temperature in VO_2, as detailed in Table 6.

Table 6. Thermochromic Performance of VO_2 Based on Hybrid Structure.

Category	Material/Structure	$T_{_lum}$ (%)	$\Delta T_{_sol}$ (%)	$T_{_\tau}$ (°C)	Reference
Element Doping	Si-doped VO_2 film	54.7	13.9	NR	[149]
	Zr-doped VO_2 film	61.4	10.3	NR	[150]
	Mg-doped VO_2 film	59.4	9.5	NR	[150]
	W-doped VO_2 film	54.4	10.7	39.0	[151]
	W-doped VO_2 coating	45.0	10.0	22.0	[152]
	H-doped VO_2	NR	NR	30.0	[153]
	W/Zr co-doped VO_2 film	48.4	2.0	36	[154]
	W/Mg co-doped VO_2 film	46.2	10.8	36.9	[155]
	Hf/W co-doped VO_2 film	41.1	13.1	38.9	[156]
	SiO_2/W co-doped VO_2 film	48.5	NR	NR	[157]

6.1.3. Multilayer Structures

Multilayer structures typically consist of "dielectric/VO_2/dielectric" or more complex sandwich structures, enabling precise tuning of spectral selectivity and overall optical performance through effects such as reflection–transmission interference, refractive index gradients, and interfacial scattering. Through rational design of multilayer sandwich structures, the bottom layer can serve as a buffer to improve film stress and crystalline quality, while the top layer functions as an anti-reflective coating to enhance visible light

transmittance or near-infrared reflectance. These design strategies significantly improve the overall performance of VO_2 films in smart window applications [160,161].

Research employing pulsed laser deposition has demonstrated the efficacy of multilayer structures in regulating optical constants and phase structures, with BN films serving as both buffer and anti-reflective layers within BN/VO_2/BN sandwich architectures [162].

Although multilayer structures impose higher demands on process precision and thickness control during fabrication, potentially increasing costs, they offer greater flexibility for performance optimization. This makes them well-suited for customized designs tailored to diverse application scenarios.

In practical applications, multilayer structural strategies achieve comprehensive optimization of $T_{_lum}$ and $\Delta T_{_sol}$ through composite interlayers of varying types. For instance, a five-layer structure comprising $TiO_2/VO_2/TiO_2/VO_2/TiO_2$ realized 12.1% solar modulation capability and 45.0% visible light transmittance [163]. A more complex multilayer structure, SiN_x/NiCr/$NiCrO_x$/VO_x/$NiCrO_x$/NiCr/SiN_x, exhibits a relatively low $T_{_lum}$ of 40.5% while achieving a high $\Delta T_{_sol}$ of 18.4%, indicating excellent solar modulation performance [164].

Relatively simple three-layer structures such as $SiN_x/VO_2/SiN_x$ [165] and $SiO_2/VO_2/SiO_2$ [166] also demonstrate outstanding performance. The former achieves high light transmittance while maintaining over 14.5% solar modulation capability, whereas the latter attains a $T_{_lum}$ as high as 54.0%. Furthermore, the $WO_3/VO_2/WO_3$ tri-layer structure achieves a $T_{_lum}$ of 55.4%, combining substantial modulation capability with good light transmission [167], as shown in Table 7.

Table 7. Thermochromic Performance of VO_2 Based on Multilayer Structure Strategy.

Category	Material/Structure	$T_{_lum}$ (%)	$\Delta T_{_sol}$ (%)	$T_{_\tau}$ (°C)	Reference
Multilayer Film	VO_2/TiO_2 bilayer film	61.5	15.1	NR	[158]
	Si-Al/VO_2 bilayer coating	44.0	18.9	NR	[159]
	$TiO_2/VO_2/TiO_2/VO_2/TiO_2$ multilayer film	45.0	12.1	54.0	[163]
	SiN_x/NiCr/$NiCrO_x$/VO_x/$NiCrO_x$/NiCr/SiN_x multilayer film	40.5	18.4	NR	[164]
	$SiN_x/VO_2/SiN_x$ multilayer film	40.4	14.5	NR	[165]
	$SiO_2/VO_2/SiO_2$/polymer multilayer coating	54.0	16.4	NR	[166]
	$WO_3/VO_2/WO_3$ multilayer structure	55.4	NR	52.0	[167]

Overall, multilayer designs not only enhance optical performance but also enable the incorporation of additional functionalities such as weather resistance, self-cleaning, and hydrophilicity in the shell or outer layers, thereby offering significant potential for energy-efficient buildings and outdoor applications.

6.1.4. Nanostructures

Nano-structural regulation primarily enhances VO_2's phase transition behavior and optical response at dual scales—crystalline and geometric—through grain size reduction and micro-morphology adjustment. On the one hand, nanocrystals possess large specific surface areas and high surface energies, while partially relaxing lattice constraints present in bulk materials. This effectively lowers phase transition barriers, thereby reducing phase transition temperatures. On the other hand, distinctive nanomorphologies (such as porous, networked, columnar, and micro-patterned structures) enhance scattering and absorption of near-infrared light. This amplifies transmission differences between high- and low-temperature states, significantly boosting solar modulation efficiency. Furthermore, nanostructures can buffer volumetric stresses generated during phase transitions,

mitigating failure behaviors such as film cracking and delamination, thereby improving cycling stability.

In the design of nanocomposite films, common strategies involve combining VO_2 nanoparticles with other functional nanoparticles or dispersing them within a polymer matrix to achieve flexible or coatable thermochromic coatings, as detailed in Table 8. For instance, compositing VO_2 nanoparticles with Sb-doped SnO_2 (ATO) nanoparticles enhances solar light modulation capability ($\Delta T_{sol} \approx 20.0\%$) while achieving T_{lum} of 60.1%. Furthermore, dispersing VO_2-based nanoparticles within a polyurethane matrix and constructing a three-layer structure maintains $\Delta T_{sol} \approx 20.0\%$ while ensuring adequate mechanical flexibility. Core–shell nanoparticle designs similarly demonstrate significant potential; for example, VO_2@SnO_2 core–shell nanoparticles achieve ΔT_{sol} of 25.0%, delivering substantial infrared modulation effects while maintaining high transmittance.

Table 8. Thermochromic Performance of VO_2 Based on Nanostructure Strategy.

Category	Material/Structure	T_{lum} (%)	ΔT_{sol} (%)	T_{τ} (°C)
Nanocomposite Film	VO_2 nanoparticles in Ni-based thermochromic system	73.4	18.2	NR
	VO_2 nanoparticles with Sb-doped SnO_2 nanoparticles	60.1	20.0	66.3
	VO_2 nanoparticles with Sb-doped SnO_2 nanoparticles	84.4	11.6	84.5
	HfO_2/VO_x nanocomposite film	51.6	15.4	60.6
	VO_2 nanoparticles/SiO_2 aerogel composite film	41.2	18.4	NR
	VO_2 nanoparticles/PU composite film (single layer)	54.0	14.5	NR
	VO_2 nanoparticles/PU composite film (triple layer)	46.8	20.0	NR
	VO_2 nanoparticles/PVB composite film	43.4	17.3	NR
	VO_2(M)@SnO_2 core–shell nanoparticles	47.5	25.0	~65.0
	VO_2 nanoparticles/PVP composite film	57.3	13.8	NR
	W-doped VO_2 nanoparticle film	50.0	10.0	32.0
	VO_2 bilayer nanoparticle array	46.1	13.2	NR
Nanostructure/Microstructure	3D ordered macroporous VO_2 film	71.1	10.8	NR
	Nanoporous VO_2-based film	78.0	14.1	NR
	VO_2 nanoparticle film with VO_2 clusters	46.3	11.2	NR
	VO_2 mesh film	86.0	NR	NR
	Micro-patterned VO_2 thermochromic film	43.3	14.9	NR

Conversely, constructing three-dimensional ordered microporous VO_2 or nanoporous VO_2 films leverages the anti-reflective properties of porous structures to substantially enhance T_{lum}, achieving visible light transmittances of 71.1% and 78.0%, respectively. The T_{lum} of VO_2 reticular films can be further elevated to 86.0%, while micro-patterned VO_2 films maintain stable solar modulation capability (ΔT_{sol} = 14.9%).

These studies demonstrate that meticulous design of composite methods and geometric morphologies of VO_2 at the nanoscale offers a promising approach to overcoming the traditional trade-off between light transmittance and modulation capability in dense films.

To date, numerous methods have been developed for the preparation of VO_2-based nanoparticles and films. Prominent techniques for fabricating thermochromic VO_2 nanostructures include hydrothermal synthesis, magnetron sputtering [168], chemical vapor deposition (CVD) [169], and sol–gel processes [170]. From a reaction mechanism perspective, these methods can be broadly categorized into chemical and physical approaches. For industrial applications, factors such as cost, scalability, and equipment complexity are particularly critical. Consequently, chemical solution methods and physical sputtering techniques have received greater attention, and research on these methods has been relatively focused.

6.2. Process Optimization

Once the material composition and structural design are established, careful control of preparation parameters can significantly enhance the overall performance of TCMs. Broadly, preparation techniques encompass chemical solution methods and physical vapor deposition/sputtering methods, each exhibiting distinct characteristics regarding film formation mechanisms, crystalline quality, cost, and scalability.

6.2.1. Process Optimization—Chemical Solution Method

Chemical solution methods synthesize TCMs through chemical reactions or phase transitions within solutions. Typical approaches include sol–gel synthesis and hydrothermal or hydrothermal-solvothermal processes. Such methods generally offer advantages including simple equipment, lower processing temperatures, and flexible composition control, making them suitable for large-area coatings or bulk powder preparation. However, the crystallinity and phase purity of the resulting materials often depend on subsequent thermal treatments such as annealing. Improper control of process parameters may lead to phase impurities or uneven grain size distribution, causing performance fluctuations.

Among these, the hydrothermal method is commonly employed for synthesizing high-quality nanoscale VO_2(M), offering both large-scale production capability and precise phase structure control [171]. Under relatively mild hydrothermal conditions, pentavalent vanadium compounds such as V_2O_5 or NH_4VO_3 are used as precursors, with reducing agents such as oxalic acid [172], diaminohydrochloric acid, or ethylene glycol [173] introduced. Uniform precipitation of intermediate species like $VOSO_4$ enables the synthesis of vanadium oxides with desirable phase compositions. However, due to the existence of multiple polymorphs in the VO_2 system and its complex phase diagram, hydrothermal products frequently form metastable or multiphase coexistence structures rather than pure VO_2(M), complicating preparation [174].

Recent studies have made significant progress in controlling size, morphology, and phase structure of VO_2 for energy-saving window materials, enabling low-temperature and controllable preparation. Zhao et al. [175] employed a one-step hydrothermal approach using hydrazine as both a reducing and structure-directing agent to generate oxygen vacancies in situ. This reduced the phase transition temperature from 68 °C to 50 °C and, through precise control of spherical nanoparticle sizes (32–46 nm), prevented grain growth during high-temperature annealing, synergistically enhancing optical properties ($T_{_lum}$ = 43.4%, $\Delta T_{_sol}$ = 17.3%).

Molloro et al. [176] used Ethiopian banana fiber as a template to synthesize a three-dimensional mesoporous structure assembled from VO_2 nanosheets. The mesoporous scattering and low refractive index increased visible light transmittance to 67.3%, while the continuous VO_2 network ensured $\Delta T_{_sol}$ of 12.5%. Nanoplate surface effects further reduced the phase transition temperature to 63.15 °C. Zhang et al. [177] employed high-temperature, high-pressure hydrothermal conditions to generate highly crystalline, low-defect VO_2(M) nanoparticles. This approach enabled uniform W atom doping, lowering the phase transition temperature near room temperature and controlling particle sizes between 20–50 nm.

Wang et al. [178] synthesized VO_2(D) precursors hydrothermally and converted them to VO_2(M) via annealing at 250 °C. This suppressed grain growth, yielding small nanoparticles (20–30 nm), lowering $T_{_\tau}$ to ~62 °C, and improving solar modulation efficiency ($\Delta T_{_sol}$ up to 11.9%). Chang et al. [179] developed a controlled-oxygen hydrothermal method. By precisely regulating oxygen partial pressure and precursor concentration, they achieved one-step synthesis of stoichiometric, size-controlled (25–52 nm) VO_2(M) nanocrystals, enhancing optical properties of flexible films ($T_{_lum}$ = 66.42%, $\Delta T_{_sol}$ = 19.2%).

Guo et al. [180] synthesized a VO_2(B) precursor with uniform W/Zr doping and a distinctive dandelion/petal morphology under high-temperature and high-pressure hydrothermal conditions. This precursor laid the structural and compositional foundation for VO_2 materials with low phase transition temperature (via W doping), high visible light transmittance, and high solar modulation capability (via Zr doping), achieving synergistic performance optimization [181]. These advances demonstrate that hydrothermal methods enable precise control over VO_2 nanostructures, overcoming limitations of conventional high-temperature solid-state reactions.

6.2.2. Process Optimization—Physical Vapor Deposition

Physical vapor deposition employs high-energy ions or plasma to bombard a target material, causing atoms or molecules to sputter off and deposit onto a substrate surface to form a thin film. Films prepared using this method typically exhibit high purity and crystallinity, along with precise control over composition, thickness, and microstructure. It is particularly suitable for producing dense, uniform, and highly reproducible VO_2 films. By contrast, its drawbacks include substantial equipment investment, complex process parameters, stringent operational requirements, and limitations regarding substrate size compatibility.

Current physical techniques commonly used for preparing VO_2 thin films include magnetron sputtering, pulsed laser deposition (PLD), atomic layer deposition (ALD), and electron beam evaporation. Among these, magnetron sputtering has become one of the most widely adopted approaches for fabricating multilayer VO_2 films due to its advantages in film uniformity, density, and large-area scalability. Compared with other physical methods, magnetron sputtering offers higher deposition efficiency and excellent compatibility with existing industrial coating lines.

Jin et al. [100] employed magnetron sputtering to fabricate ZnO/VO_2/ZnO multilayer films. The bottom ZnO buffer layer effectively improved the crystalline quality of VO_2, increasing its $\Delta T_{_sol}$ to 13.5%. The top ZnO anti-reflective layer further enhanced the $T_{_lum}$ to approximately 50%. The resulting dense and uniform films provide a solid foundation for practical VO_2 smart-window applications.

Victor et al. [182] also used magnetron sputtering to deposit VO_2/W multilayer films. Appropriate post-annealing enabled precise and uniform W doping in VO_2, effectively lowering the phase transition temperature to approximately 21 °C while maintaining a high infrared modulation ratio of 68.4% and narrowing the thermal hysteresis width to about 5 °C. These improvements significantly enhanced the sensitivity and stability of the thermochromic response.

Savorianakis et al. [183] employed reactive magnetron sputtering combined with grazing-incidence deposition (GLAD) to produce high-purity VO_2 films with tilted or upright nanostructures. Precise stoichiometry control enabled stable nanostructure formation, resulting in markedly improved thermochromic performance, including more than doubled infrared modulation capability, increased visible light transmittance, a broader phase-change hysteresis window, and pronounced optical anisotropy.

Ho et al. [184] used V_2O_5 as the target material and prepared VO_2 films via magnetron sputtering coupled with in situ annealing. By precisely regulating the oxygen flow, they directly obtained high-purity, well-crystallized VO_2 films on non-epitaxial substrates. Owing to their large grain size and low defect density, the films exhibited excellent thermochromic performance: an infrared modulation rate of 77%, solar modulation efficiency of 5.87%, thermal hysteresis width of approximately 5.75 °C, and resistivity changes spanning nearly two orders of magnitude.

Zhan et al. [185] combined room-temperature magnetron sputtering with rapid thermal annealing to fabricate VO_2 films. By constructing a $SiN_x/NiCrO_x$ multilayer structure, they achieved significant enhancements in thermochromic performance ($\Delta T_{_sol}$ reaching 18.02%), reduced the phase transition temperature to around 54 °C, and improved oxidation resistance up to 375 °C. Meanwhile, annealing times were shortened by approximately 75%, markedly improving production efficiency and operational safety.

Vu et al. [186] further employed high-power pulsed magnetron sputtering (HiPIMS) to deposit highly crystalline, high-purity VO_2 films onto soda–lime glass at a deposition rate of approximately 5.7 $nm \cdot min^{-1}$. The high-energy particle flux improved film density and quality, achieving a maximum solar modulation rate of approximately 12% while effectively suppressing substrate-induced impurity diffusion. This advancement represents a noteworthy step towards practical implementation of VO_2 smart windows.

Overall, existing studies consistently demonstrate that magnetron sputtering has received greater attention than other physical techniques in VO_2 synthesis and thin-film engineering, establishing itself as a key technological pathway for producing high-quality thermochromic VO_2 films.

6.3. Green TCMs

In this paper [187], green TCMs are defined according to three main criteria: they are derived from renewable or bio-based sources, exhibit good biodegradability, and show minimal toxicity during use and disposal. Based on this understanding, current studies have mainly focused on replacing conventional matrices with biodegradable, bio-based, or low-toxicity alternatives, while also trying to reduce the environmental burden associated with dyes and auxiliary components.

Even so, developing a truly green thermochromic system is still far from straightforward. In most cases, the matrix may be improved first, but the chromophore, solvent system, or processing additives may still limit the overall environmental performance. For this reason, many of the materials reported so far are better described as greener formulations rather than fully sustainable systems.

Even with these limitations, the progress made so far is still meaningful. Biodegradable polymer matrices, natural pigments, and lower-toxicity dye systems have already been introduced into thermochromic composites, especially for packaging, wearable indicators, and temperature-sensing textiles. These attempts show that environmental compatibility can be improved without completely sacrificing thermochromic functionality. The difficulty is that greener choices often come with trade-offs. Natural colorants may suffer from poor thermal stability and photobleaching, while biodegradable matrices may show weaker water resistance, lower mechanical robustness, or gradual performance loss during repeated heating and cooling. Likewise, greener solvent systems such as aqueous media or other low-volatility alternatives can reduce environmental burden, but they often make formulation control and large-scale processing more difficult.

Looking ahead, the real challenge is not simply replacing one component with a greener one, but finding a workable balance between environmental compatibility and material performance. A useful green TCM should still maintain reliable reversibility, clear color contrast, an appropriate response temperature, and acceptable long-term stability.

6.4. Summary of Promising Strategies for Addressing Key Challenges

Although TCMs have been studied extensively, several issues still limit their wider use. For VO_2-based systems, the most familiar ones are the high phase-transition temperature, low visible-light transmittance, and the difficulty of improving transparency without

weakening solar modulation. Durability under real service conditions is another concern, especially for coatings and window-related applications.

Among the reported approaches, elemental doping is still the most straightforward way to reduce the phase-transition temperature. Tungsten is the dopant most often used for this purpose, and other single- or co-doping strategies have also been explored. Even so, lowering the transition temperature does not automatically solve the whole problem. In some cases, heavy doping weakens the thermochromic response or leads to poorer optical quality. This is why doping is useful, but usually not sufficient on its own.

When the main goal is to improve visible transmittance while keeping reasonable solar modulation, multilayer and composite designs tend to work better. Additional layers can act as antireflection coatings, optical-interference layers, or protective barriers, which makes it easier to tune transparency and infrared regulation at the same time. For smart windows, these designs are often more practical than relying on composition adjustment alone.

Core–shell structures and nanostructure regulation offer another route, especially when long-term stability matters. A suitable shell can help protect VO_2 from oxidation and moisture, while nanoscale structural control can reduce transition barriers and improve switching behavior during repeated cycling. In that sense, these approaches help not only with performance, but also with service reliability.

Overall, no single strategy solves all of the main limitations at once. Doping is mainly useful for lowering the phase-transition temperature, whereas multilayer and composite structures are more effective for improving optical balance. Core–shell and nanostructured designs are particularly helpful for stability and durability. For practical applications, the most promising direction is therefore to combine these strategies according to the needs of the specific device or use scenario.

7. Application and Performance Analysis of TCMs

TCMs have attracted broad interest because temperature-induced structural or molecular changes can be directly translated into useful optical responses. In practice, however, this translation is not automatic. A thermochromic mechanism is only valuable when it can provide the kind of switching behavior required in a specific application, such as near-room-temperature operation for smart windows, clear visual contrast for temperature indicators, rapid response for sensors, or sufficient flexibility and durability for wearable and flexible devices.

The following sections will discuss the working principles, application performance, major challenges, and potential strategies for enhancing TCMs across several representative application scenarios.

7.1. Thermochromic Smart Windows

TCMs are among the most widely studied materials for energy-saving window applications. Over the past several decades, architectural glazing aimed at reducing building energy consumption has progressed rapidly. With advances in thermochromic coatings and thin-film fabrication, thermochromic windows have become a promising option for high-performance façades and exterior glazing systems [20,188].

Among inorganic TCMs, vanadium oxides—particularly vanadium dioxide (VO_2)—have been the focus of the most intensive research. The thermochromic behavior of VO_2 was first reported in 1959 [189]. Near its critical $T_{_\tau}$, VO_2 undergoes a remarkable and reversible structural transition from a monoclinic semiconducting phase to a tetragonal metallic phase. Below $T_{_\tau}$, VO_2 remains in the monoclinic state, displaying semiconducting properties and allowing high transmittance of near-infrared (NIR) radiation. Once heated

above $T_{_\tau}$, it transforms into the metallic phase, exhibiting strong NIR reflectance and thereby markedly reducing solar heat gain [190], as detailed in Table 9.

Table 9. Radiative Properties of VO_2-Coated Glass and Ordinary Glass.

Property	VO_2-Coated Glass		Ordinary Glass
	Semiconducting State	Metallic State	
Solar Absorptance	0.482	0.590	0.159
Solar Reflectance	0.078	0.055	0.070
Solar Transmittance	0.440	0.335	0.771
Longwave Emissivity	0.880	0.880	0.840
Luminous Transmittance	0.435	0.421	0.837

This reversible phase transition is accompanied by dramatic changes in optical and electrical properties, including a conductivity variation spanning several orders of magnitude near room temperature. Such attributes endow VO_2-based thermochromic glazing with significant potential for smart building applications, enabling passive energy regulation, dynamic solar modulation, and adaptive indoor thermal management.

From a device-architecture perspective, thermochromic glazing can be realized through a variety of coating and lamination strategies. A particularly promising approach involves incorporating TCMs directly into polyvinyl butyral (PVB) to form thermochromic interlayers, which are subsequently laminated with glass. This technique is compatible with existing laminated safety glass and acoustic glass production lines, thereby facilitating large-scale industrialization [191]. In parallel, VO_2 thin films can be deposited via multiple physical and chemical vapor deposition methods—including chemical vapor deposition (CVD), pulsed laser deposition (PLD), magnetron sputtering, and sol–gel processing. Precise regulation of processing parameters and microstructural evolution enables extensive tuning of film color appearance, spectral selectivity, and thermochromic switching behavior. Moreover, nano/microstructural engineering affords significant opportunities for further enhancing device performance.

As a representative thermochromic glazing technology, VO_2-based smart windows dynamically modulate solar heat gain in response to ambient temperature fluctuations [192]. However, from a building-application perspective, the optimal switching temperature should not be treated as a fixed material constant alone. In practice, the preferred switching threshold depends strongly on the local climate, seasonal operating conditions, and façade orientation. For example, glazing exposed to intense solar radiation or west-facing afternoon sun may require earlier solar control, whereas in colder climates or on less solar-exposed façades, an excessively low switching temperature may undesirably reduce passive solar heat gain during heating seasons. Therefore, the target transition temperature for smart-window materials should be evaluated in relation to real climatic conditions and façade-specific thermal loads, rather than being discussed only as an intrinsic materials parameter.

To address these limitations, multiple optimization pathways have been proposed. Doping remains the most straightforward and effective strategy for lowering $T_{_\tau}$, with W^{6+} doping capable of reducing the transition temperature by approximately 20–28 K at atomic-level concentrations [193–196]. In addition, intrinsic structural optimization—achieved by tuning grain size, porosity, and crystallographic morphology [197]—and extrinsic structural engineering—such as constructing core–shell architectures, hybrid nanostructures, and multilayer composite films [198,199]—can further enhance the thermochromic response. Compared with relying solely on intrinsic optimization, compositing VO_2 with organic or inorganic materials offers greater flexibility and often yields a more balanced enhancement

of $T_{_lum}$, $\Delta T_{_sol}$, and $T_{_\tau}$, while simultaneously providing additional functionalities such as improved weather resistance, self-cleaning behavior, or hydrophilicity [200].

Another important issue in real deployment is that thermochromic switching in windows is rarely fully uniform or simply binary. In practice, the optical response is jointly influenced by solar irradiance, outdoor air temperature, indoor set-point temperature, wind conditions, and heat transfer through the glazing system. Under such combined conditions, partial switching may occur across the window area or during intermediate states, which can significantly affect both solar heat-gain control and visual appearance. In addition, hysteresis width is highly relevant for building use: an excessively broad hysteresis may delay recovery during cooling or trigger asymmetric behavior during heating and cooling cycles, leading to a mismatch between the actual optical state and the desired thermal-control demand. For this reason, hysteresis width, switching sharpness, and intermediate-state behavior should be considered together when evaluating the practical suitability of smart windows.

Beyond VO_2, poly(N-isopropylacrylamide) (PNIPAM) hydrogels represent another key class of TCMs under investigation for smart window applications. PNIPAM exhibits a low transition temperature (~32 °C), excellent flexibility, and good biocompatibility, making it suitable for low-temperature response systems and wearable devices. However, it suffers from slow response kinetics, limited mechanical robustness, and suboptimal environmental stability. In contrast, VO_2 films rely on crystalline structural transitions, enabling rapid and reversible near-infrared modulation at approximately 68 °C with high mechanical integrity and environmental resistance—properties that make them more suitable for architectural glazing and high-temperature thermal management [20]. Each system offers unique advantages, and rational integration—for example through VO_2/polymer composite films—can effectively combine flexible processability with strong optical regulation capabilities.

In addition to energy-saving performance, user acceptance is also critical for architectural smart windows. In practical use, the evaluation of thermochromic glazing should include not only luminous transmittance and solar modulation, but also glare control, color neutrality, color rendering, and overall aesthetic acceptability. A window that provides strong solar regulation but introduces a pronounced yellow or brown tint, excessive haze, or non-uniform color appearance may face resistance in real building applications even if its thermal performance is favorable. These aspects are commonly assessed through visible transmittance spectra, CIE L*a*b* color coordinates, color difference analysis, and where possible, daylight and occupant-comfort evaluations. Future studies on smart windows should therefore pay greater attention to balancing thermal regulation with visual comfort and architectural acceptability.

Durability and long-term reliability are also central to the feasibility of smart-window deployment. Under outdoor service conditions, thermochromic layers may suffer from oxidation, hydrolysis, interfacial delamination, cracking caused by thermal expansion mismatch, gradual loss of optical contrast, irreversible drift in switching temperature, surface abrasion, and degradation induced by cleaning agents or environmental pollutants. Accordingly, application-oriented evaluation should extend beyond short-term optical measurements and include representative accelerated-aging tests, such as repeated thermal cycling, ultraviolet exposure, combined heat–humidity aging, abrasion resistance, and chemical resistance to routine cleaning conditions. Only by combining optical performance with durability testing can the long-term practicality of thermochromic smart windows be assessed more realistically.

In terms of safety considerations, Xu et al. [201] emphasized that VO_2-based smart windows are deployed in everyday environments and are directly accessible to the public, making material safety a critical concern. The potential toxicity associated with VO_2 mainly

arises from two aspects. First, vanadium and its compounds intrinsically exhibit a certain level of toxicity. The physicochemical properties and aging behavior of VO_2 nanoparticles significantly influence their toxicological profile, as aging may lead to increased release of V ions [202]. These ions can be introduced into the environment during material synthesis, long-term use, or disposal and recycling processes. Second, the VO_2 surface is prone to microbial colonization. Biofilms formed by microorganisms may gradually degrade the coating and, in some cases, present risks to human health.

To mitigate these issues, incorporating functional layers—such as TiO_2—onto VO_2 coatings [6] has been shown to not only enhance optical performance and impart self-cleaning characteristics but also improve resistance to microbial contamination. TiO_2 layers provide photocatalytic activity that suppresses biofouling, thereby offering a dual function of performance enhancement and biological protection.

Looking ahead, future research should focus on systematically assessing the full life-cycle safety of VO_2-based smart windows, incorporating toxicological evaluation, environmental fate analysis, and anti-biofouling performance. Moreover, the development of environmentally benign, low-toxicity, or alternative TCMs will be essential for advancing the sustainable and safe deployment of smart window technologies.

The practical value of thermochromic smart windows should be judged not only by intrinsic material parameters, but also by their climate adaptability, façade-dependent operating behavior, visual comfort performance, and long-term service reliability in real building environments.

7.2. Temperature Indicators

TCMs can be employed to fabricate a wide range of temperature-indicating devices, including temperature labels, thermochromic stickers, and time–temperature integrator labels. These indicators function by exhibiting reversible or irreversible color changes within predefined temperature ranges, enabling the monitoring of temperature histories for food, beverages, pharmaceuticals, and biological products during storage and transportation. Such color responses allow the rapid identification of temperature excursions beyond safe limits, thereby supporting quality control and risk assessment. In these devices, TCMs typically undergo temperature-driven phase transitions, molecular conformational changes, or rearrangements of hydrogen-bonding networks, which modify their spectral absorption characteristics and ultimately generate observable color differences.

Reference [203] further proposes integrating mechanoresponsive polymer concepts into thermochromic design by incorporating stress-activatable covalent bond units into polymer backbones or side chains. This enables color changes triggered by external mechanical forces or deformation. When combined with temperature fields, such dual-responsive systems offer promising opportunities for developing multifunctional temperature-indicating devices capable of detecting both thermal and mechanical perturbations.

Currently, low-temperature reversible TCMs that have been widely investigated fall mainly into three categories. The first comprises poly(diacetylene) (PDA) conjugated polymers [204,205]. The second includes organic natural pigments such as anthocyanins [36,206] and curcumin [207]. The third consists of ternary TCMs, composed of a phase-transition temperature regulator (PTS), a chromophore, and a color suppression agent [208,209]. Among these systems, TCMs have gained considerable attention in temperature-sensitive labeling and cold-chain monitoring due to their tunable color and transition temperature, high sensitivity, and relatively low cost [210,211].

Poly(diacetylene) (PDA) represents a family of conjugated organic polymers with an ethene–acetylene alternating backbone. When exposed to external stimuli such as heat [212], electrical current [213], ions [214,215], or biomolecules [216], PDA undergoes

a distinct color transition from blue to red. This makes PDA one of the most prominent research hotspots in the field of stimuli-responsive color-changing materials. PDA can be efficiently synthesized via solid-state polymerization of diacetylene monomers under 254 nm ultraviolet irradiation, typically within minutes. Its thermochromic properties are strongly determined by the chemical structure and aggregation behavior of the monomer precursors [217,218]. Studies have demonstrated that incorporating aromatic and/or hydrogen-bonding functional groups into the monomer modifies intermolecular interactions and molecular packing, which in turn influence polymerization kinetics and the thermochromic transition temperature of the resulting PDA.

Polydiacetylenes (PDAs) represent a prominent class of organic thermochromic polymers. As explicitly illustrated in Figure 2, the formation and color transition of PDA follow a highly ordered topochemical process. Initially, closely packed diacetylene (DA) monomers undergo 1,4-addition polymerization upon UV irradiation (254 nm) without the need for any catalyst. This process yields a highly conjugated, planar eneyne backbone that absorbs broadly around 640 nm, thus exhibiting a strong blue appearance (Blue-phase PDA). Upon thermal stimulation, the planar conjugated backbone undergoes a distinct conformational distortion. This thermally induced twisting disrupts the effective conjugation length of the polymer chains, shifting the maximum absorption to approximately 540 nm and leading to a rapid macroscopic color transition from blue to red (Red-phase PDA). Due to this intuitive and naked-eye-visible response, PDAs are highly favored for thermal indication and passive smart sensors.

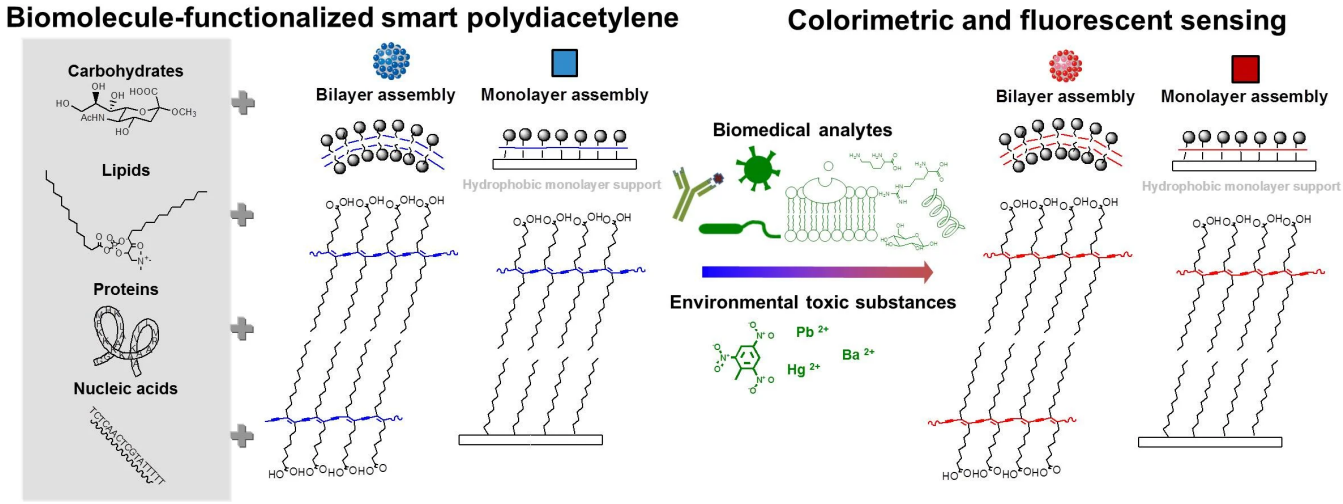


Figure 2. Schematic representation of the 1,4—addition photopolymerization of diacetylene (DA) monomers into blue—phase polydiacetylene (PDA) under UV irradiation, and the subsequent thermally induced backbone distortion leading to the red-phase transition. Reproduced from Ref. [219] under the terms of the Creative Commons CC–BY license.

Regarding ternary thermochromic systems, Shi et al. [220] conducted a systematic screening of organic compounds containing long alkyl chains to evaluate their phase-transition temperatures (PTTs) and thermal stability, thereby optimizing the phase-transition subsystem (PTS) within TTM formulations. They further investigated the effects of different chromogenic agents on the thermochromic stability and reversibility of TTM systems. Through this comprehensive analysis, the authors successfully developed a stable low-temperature reversible thermochromic indicator (LT-RTI) tailored for monitoring the storage and transportation conditions of temperature-sensitive products.

This LT-RTI exhibited clear and distinguishable color changes within the temperature ranges of 6–8 °C and −23 to −18 °C, enabling effective visual monitoring of temperature

excursions during cold-chain logistics. Notably, the indicator demonstrated strong applicability for the storage requirements of oral polio vaccine (OPV) and inactivated polio vaccine (IPV), providing a reliable, real-time visualization tool for ensuring vaccine temperature safety throughout distribution.

7.3. Anti-Counterfeiting Markings

Thermochromic printing inks have gained increasing traction in smart packaging, anti-counterfeiting technologies, and interactive marketing, particularly in applications that emphasize product uniqueness and added value [24]. Whereas traditional inorganic thermochromic pigments have seen limited color variety and tunability, modern formulations predominantly rely on organic color-developing polymer systems. These organic thermochromic inks provide a broad palette of colors and allow precise control over transition temperatures and color-change intervals, making them especially attractive for high-security applications such as banknotes, identification documents, and premium product packaging.

In anti-counterfeiting printing, the essential working principle of thermochromic inks is their reversible and temperature-dependent color response. Rahela et al. [24] systematically evaluated the colorimetric properties of red, blue, black, and colorless thermochromic inks with an activation temperature of 31 °C. Colorless dye-based inks were found to appear colored at lower temperatures and transition to a colorless state upon heating. Their chromatic behavior is not only determined by instantaneous temperature but also exhibits pronounced thermal hysteresis, strongly influenced by the ink's prior thermal exposure. As a result, noticeable color discrepancies arise at identical temperatures during heating and cooling cycles. While this phenomenon enables partial recording of temperature history, it simultaneously poses additional challenges for long-term formulation stability. Indeed, limited durability and insufficient aging resistance remain major bottlenecks hindering broader adoption of thermochromic anti-counterfeiting inks.

To address the durability issue, self-healing functional materials have recently been incorporated into thermochromic ink design. Gouda et al. [221] developed a thermochromic anti-counterfeiting ink based on self-healing anthocyanin composite hydrogels. By integrating anthocyanin extracts and $FeSO_4$ into CNF@PLA self-healing hydrogels, they fabricated a series of color-tunable, temperature-responsive composite hydrogels. These thermochromic CNF@PLA hydrogels can be used for stamping official documents such as passports, banknotes, and certificates, with their color-change behavior directly governed by the anthocyanin concentration. Experimental results show that stamped paper appears purple at approximately 25 °C (absorption peak ~614 nm) and shifts to a reddish-purple color at 60 °C (absorption peak ~449 nm).

This study provides a new conceptual pathway for designing low-cost, environmentally friendly, and self-healing thermochromic anti-counterfeiting inks, highlighting their potential value not only in high-security authentication but also in temperature-monitoring applications.

Leveraging their reversible color change and ability to record thermal history, thermochromic anti-counterfeiting materials can be deployed across diverse fields including currency, security credentials, premium packaging, and logistics labeling. Through rational design of transition temperatures, color combinations, and spatial arrangement of patterns, manufacturers can construct multi-tier, multidimensional anti-counterfeiting systems that substantially increase replication difficulty, reduce the risk of forgery, protect consumer rights, and maintain market integrity.

7.4. Temperature Sensors

Beyond visual indication and anti-counterfeiting, TCMs also demonstrate broad potential in temperature sensing and thermal management. By incorporating thermochromic components into flexible substrates, coatings, or fibers, it is possible to develop passive temperature sensors capable of both visual temperature indication and thermal regulation. Such systems are particularly suitable for real-time monitoring of temperature variations on equipment surfaces, human skin, and ambient environments. When the temperature reaches a predefined threshold, the material undergoes a spontaneous color transition, providing an intuitive visual signal that can prompt timely control actions or protective responses.

Figure 3 illustrates the structural design and preparation of stretchable thermochromic fibers for smart fabric applications. By encapsulating phase-change thermochromic materials within a highly elastic polymer matrix (such as polyurethane), these smart fibers exhibit excellent mechanical stretchability alongside a reversible visual color response to temperature variations. Such flexible integration allows these fibers to be easily woven or knitted into everyday garments. This capability not only ensures conformal contact with the human body but also highlights the immense potential of thermochromic composites in next-generation smart textiles, wearable electronics, and personal thermal.

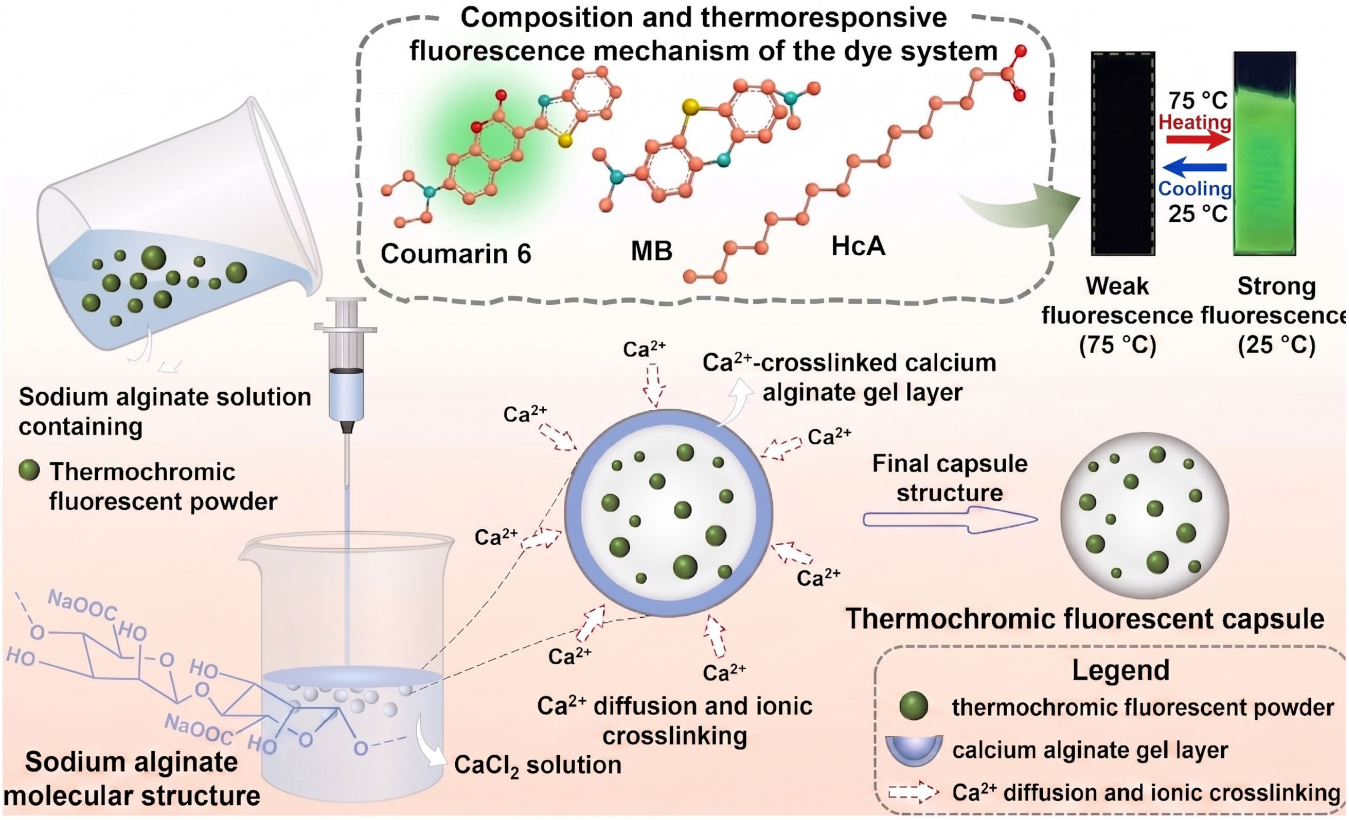


Figure 3. Schematic illustration of the structural design and fabrication of stretchable thermochromic fibers. The smart fibers can be integrated into textiles, exhibiting high mechanical stretchability and reversible visual color transitions upon thermal stimulation. Reproduced from Ref. [222].

Other researchers such as He et al. [223] prepared a class of thermochromic micro/nanoscale phase-change materials (TC-M/NPCMs) with excellent energy storage capabilities and utilized them to fabricate flexible thermochromic films. On this basis, the film surface was further modified with trimethylchlorosilane (TMC) to impart hydrophobicity, enabling enhanced durability in practical environments. In terms of working mechanism,

the TC-M/NPCMs incorporated into thermochromic films serve three functions: energy storage, thermal regulation, and temperature indication. When the color-changing film is placed on the skin surface, phase-change materials (PCMs) absorb or release latent heat near their phase-transition temperature. The varying degrees of phase change in PCMs at different temperatures alter the microenvironment and the local phase state of thermochromic components within the film, thereby producing distinct colors. As documented in the literature, at an ambient temperature of approximately 26 °C, this thermochromic device was tested on the forehead, the dorsum of the hand, the wrist, and the palm. It consistently delivered clear, reproducible color responses within a brief period, enabling visualization of skin temperature variations across these regions. Featuring a simple structure and a portable design, the device requires no external power source during measurement, rendering it suitable for daily health monitoring and straightforward clinical screening.

Benefiting from the synergistic interaction between flexible substrates and phase-change materials, such thermochromic films can be directly laminated onto textiles or applied as thermal-management coatings on diverse substrates. They mitigate environmental temperature fluctuations, reduce unnecessary heat exchange, and help maintain relatively stable human skin-surface temperatures. Combining excellent heat-storage capacity with clear color readability, thermochromic phase-change films demonstrate broad application prospects in solar energy utilization, functional textiles, building insulation, packaging, and smart clothing.

7.5. Sustainability Considerations and Life-Cycle Perspective

The sustainability of TCMs should not be judged only by their energy-saving function during use. A more realistic assessment should consider the whole life cycle, including raw materials, processing conditions, service life, maintenance demand, and end-of-life handling. This is particularly important because some systems may involve metal-containing components, volatile organic substances, or fabrication routes that raise environmental and health concerns.

From this perspective, sustainability in building applications should be evaluated at the system level rather than from a single material property. Some inorganic systems offer good durability, but may still require careful safety assessment because of their composition. Organic systems may appear milder in composition, yet they can introduce other issues, such as solvent use, lower thermal stability, or limited long-term durability. Manufacturing burden also matters. Several preparation routes discussed in this review, including high-temperature synthesis, annealing, hydrothermal treatment, and vapor-phase deposition, can be energy-intensive or require tightly controlled conditions, and these factors should be considered part of the sustainability profile rather than treated as purely technical details.

The use phase is where TCMs are most likely to deliver environmental benefit, especially in smart windows and adaptive coatings for buildings. As already discussed in this review, the performance of VO_2 glazing can be linked to building energy metrics such as Energy Saving Equivalent and Energy Saving Index, which helps connect optical regulation with annual energy demand. Even so, the actual value of this benefit depends strongly on service life. If a material gradually loses performance under thermal cycling, humidity, ultraviolet exposure, or outdoor weathering, the gains achieved during use may be reduced by maintenance or replacement. End-of-life treatment also deserves more attention, since multilayer coatings and composite films are often difficult to separate, recycle, or dispose of safely. For this reason, future LCA studies should at least consider five stages: raw-material sourcing, synthesis and coating energy demand, operational energy-saving benefit, service lifetime and maintenance frequency, and end-of-life treatment. Although the available data are still not sufficient for a fully consistent comparison across all systems, a life-cycle

perspective is essential if we want to avoid overstating the sustainability of materials that perform well in optical tests but remain problematic in fabrication, durability, or disposal.

For future application-oriented assessment, a minimum LCA reporting checklist should include the following items: a clearly defined functional unit (for example, 1 m^2 of thermochromic glazing or coating over a specified service period); system boundaries covering raw-material extraction, synthesis, coating or lamination, installation, use, maintenance, and end-of-life treatment; the assumed service life and climate or operating scenario; maintenance conditions, including cleaning frequency, replacement criteria, and performance-decay assumptions; the likely end-of-life route, including separation difficulty, recyclability, reuse, landfill, or incineration; and safety-related indicators such as metal leaching, volatile emissions, and toxicity during manufacture, service, weathering, and disposal. Reporting these parameters would make sustainability claims more comparable and more useful for building applications.

8. Conclusions and Outlook

TCMs have evolved into a broad family of systems with distinct mechanisms, structures, and application targets. As discussed in the section on classification and mechanisms, inorganic systems, especially VO_2, remain the most intensively studied candidates for building-energy applications because of their temperature-triggered near-infrared regulation, while organic systems such as hydrogels offer advantages in flexibility, processability, and tunable appearance. Emerging materials, including structural-color and plasmonic systems, further expand the design space of thermochromic responses and suggest new possibilities beyond conventional color-changing routes.

The findings summarized in this review also indicate that the performance of TCMs should be evaluated through quantitative indicators rather than general descriptions alone. At the same time, the reported values vary substantially with material class, structural design, and test conditions. Selected studies have reported pronounced color contrast, substantial infrared modulation, relatively rapid switching in some hydrogel systems, and good cycling stability under specific conditions, but these results were obtained in different material systems and should not be interpreted as universal benchmark values. For clarity, the detailed numerical results are discussed in the corresponding sections of the main text together with the original references.

From a performance-enhancement perspective, the review further indicates that substantial progress has been made in addressing several intrinsic limitations of VO_2. Pristine VO_2 undergoes a phase transition near 68 °C, while selected doping, hybrid, multilayer, and nano-structuring strategies have lowered the transition temperature and improved the balance between visible transmittance and solar modulation in some reports. These advances are encouraging, but the extent of improvement remains strongly dependent on material composition, architecture, and fabrication route, and no single strategy has yet resolved all of these trade-offs simultaneously.

At the application level, these results explain why TCMs continue to attract interest for smart windows, thermal management coatings, sensing, and related adaptive devices. However, the review also makes clear that several barriers still limit wider use. Inorganic systems often still face challenges in balancing transition temperature, luminous transmittance, solar modulation, and long-term stability, while organic systems, despite their lower transition temperatures and better flexibility, often suffer from slower response, weaker mechanical robustness, and poorer environmental durability. In addition, some high-performance systems still depend on relatively complex fabrication routes, expensive processing, or potentially hazardous components, which limits large-scale deployment.

Overall, future progress in TCM research will depend less on improving any single property and more on achieving a practical balance among transition temperature, optical modulation, response speed, durability, safety, cost, and scalability. More importantly, material design needs to be connected more closely with real application requirements through mechanism-guided optimization, greener and lower-cost fabrication routes, and more standardized performance evaluation. Only in this way can TCMs move from promising laboratory materials to reliable technologies for practical use.

Author Contributions: C.C.: writing—original draft, visualization; K.H.: writing—review & editing, validation; Y.G.: data curation, formal analysis; X.H.: writing—review & editing, methodology; C.W.: project administration, supervision. All authors have read and agreed to the published version of the manuscript.

Funding: This research was supported by the National Natural Science Foundation of China (Grant No. 52308112).

Institutional Review Board Statement: Not applicable.

Informed Consent Statement: Not applicable.

Data Availability Statement: No new data were created or analyzed in this study. Data sharing is not applicable to this article.

Conflicts of Interest: Author Cong Chen is employed by the National Sciences Library (Wuhan). The remaining authors declare that the research was conducted in the absence of any commercial or financial relationships that could be construed as potential conflicts of interest.

References

1. González-Torres, M.; Pérez-Lombard, L.; Coronel, J.F.; Maestre, I.R.; Yan, D. A review on buildings energy information: Trends, end-uses, fuels and drivers. *Energy Rep.* **2022**, *8*, 626–637. [CrossRef]
2. Seyfouri, M.M.; Binions, R. Sol-gel approaches to thermochromic vanadium dioxide coating for smart glazing application. *Sol. Energy Mater. Sol. Cells* **2017**, *159*, 52–65. [CrossRef]
3. Sun, G.Y.; Cao, X.; Zhou, H.; Bao, S.; Jin, P. A novel multifunctional thermochromic structure with skin comfort design for smart window application. *Sol. Energy Mater. Sol. Cells* **2017**, *159*, 553–559. [CrossRef]
4. Zhang, J.; Wang, J.; Yang, C.; Jia, H.; Cui, X.; Zhao, S.; Xu, Y. Mesoporous SiO_2/VO_2 double-layer thermochromic coating with improved visible transmittance for smart window. *Sol. Energy Mater. Sol. Cells* **2017**, *162*, 134–141. [CrossRef]
5. Zhou, H.; Li, J.; Bao, S.; Li, J.; Liu, X.; Jin, P. Use of ZnO as antireflective, protective, antibacterial, and biocompatible multifunction nanolayer of thermochromic VO_2 nanofilm for intelligent windows. *Appl. Surf. Sci.* **2016**, *363*, 532–542. [CrossRef]
6. Zheng, S.; Xu, Y.; Shen, Q.; Yang, H. Preparation of thermochromic coatings and their energy saving analysis. *Sol. Energy* **2015**, *112*, 263–271. [CrossRef]
7. Leonard, E.; Takeda, C.; Akitsu, T. Azobenzene-Containing Schiff-Bases—Syntheses and Dyes Applications. *Colorants* **2024**, *3*, 53–72. [CrossRef]
8. Ganie, A.A.; Dar, A.A. Water Switched Reversible Thermochromism in Organic Salt of Sulfonated Anil. *Cryst. Growth Des.* **2021**, *21*, 3014–3023. [CrossRef]
9. Li, W.; Yan, X.; Zhao, W. Preparation of Crystal Violet Lactone Complex and Its Effect on Discoloration of Metal Surface Coating. *Polymers* **2022**, *14*, 4443. [CrossRef] [PubMed]
10. Vukoje, M.; Krajnović, I.; Kulčar, R.; Cigula, T.; Ivanda, K.I.; Hanzer, S.J. PCL Nanomodified Coating for the Protection of Thermochromic Prints on Packaging. *Mater. Proc.* **2023**, *14*, 51.
11. Wan, C.; Evans, Z.J.; Roxworthy, B.J.; Retzko, I.; Stephens, L.E.; Cleary, P.C.; Kats, M.A. On the Optical Properties of Thin-Film Vanadium Dioxide from the Visible to the Far Infrared. *Ann. Phys.* **2019**, *531*, 1900188. [CrossRef]
12. Ke, Y.; Wang, S.; Liu, G.; Li, M.; White, T.J.; Long, Y. Vanadium Dioxide: The Multistimuli Responsive Material and Its Applications. *Small* **2018**, *14*, 29. [CrossRef]
13. Liu, K.; Lee, S.; Yang, S.; Delaire, O.; Wu, J. Recent progresses on physics and applications of vanadium dioxide. *Mater. Today* **2018**, *21*, 875–896. [CrossRef]
14. Xu, F.; Cao, X.; Luo, H.; Jin, P. Recent advances in VO_2-based thermochromic composites for smart windows. *J. Mater. Chem. C* **2018**, *6*, 1903–1919. [CrossRef]

15. Wang, S.; Owusu, K.A.; Mai, L.; Ke, Y.; Zhou, Y.; Hu, P.; Magdassi, S.; Long, Y. Vanadium dioxide for energy conservation and energy storage applications: Synthesis and performance improvement. *Appl. Energy* **2018**, *211*, 200–217. [CrossRef]
16. Amirthalingam, S.; Rajendran, A.K.; Moon, Y.G.; Hwang, N.S. Stimuli-responsive dynamic hydrogels: Design, properties and tissue engineering applications. *Mater. Horiz.* **2023**, *10*, 3325–3350. [CrossRef]
17. Chen, Z.; Liu, J.; Chen, Y.; Zheng, X.; Liu, H.; Li, H. Multiple-Stimuli-Responsive and Cellulose Conductive Ionic Hydrogel for Smart Wearable Devices and Thermal Actuators. *ACS Appl. Mater. Interfaces* **2020**, *13*, 1353–1366. [CrossRef]
18. Seeboth, A.; Lötzsch, D.; Ruhmann, R.; Muehling, O. Thermochromic Polymers—Function by Design. *Chem. Rev.* **2014**, *114*, 3037–3068. [CrossRef]
19. Hakami, A.; Srinivasan, S.S.; Biswas, P.K.; Krishnegowda, A.; Wallen, S.L.; Stefanakos, E.K. Review on thermochromic materials: Development, characterization, and applications. *J. Coat. Technol. Res.* **2022**, *19*, 377–402. [CrossRef]
20. Cui, Y.; Ke, Y.; Liu, C.; Chen, Z.; Wang, N.; Zhang, L.; Zhou, Y.; Wang, S.; Gao, Y.; Long, Y. Thermochromic VO_2 for Energy-Efficient Smart Windows. *Joule* **2018**, *2*, 1707–1746. [CrossRef]
21. Cao, X.; Wang, N.; Law, J.Y.; Loo, S.C.J.; Magdassi, S.; Long, Y. Nanoporous Thermochromic VO_2 (M) Thin Films: Controlled Porosity, Largely Enhanced Luminous Transmittance and Solar Modulating Ability. *Langmuir* **2014**, *30*, 1710–1715. [CrossRef]
22. Hakkeem, H.M.A.; Ardra, V.S.; De, A.; Babu, A.; Padmanabhan, M.; Pillai, S. Nanocellulose-based cobalt(II) coordinated malonic acid hybrid aerogels exhibiting reversible thermochromism and moisture sensor properties. *Int. J. Biol. Macromol.* **2024**, *273*, 133140. [CrossRef]
23. Cheng, Y.; Zhang, X.; Fang, C.; Chen, J.; Wang, Z. Discoloration mechanism, structures and recent applications of thermochromic materials via different methods: A review. *J. Mater. Sci. Technol.* **2018**, *34*, 2225–2234. [CrossRef]
24. Kulčar, R.; Friškovec, M.; Hauptman, N.; Vesel, A.; Gunde, M.K. Colorimetric properties of reversible thermochromic printing inks. *Dye. Pigment.* **2010**, *86*, 271–277. [CrossRef]
25. Kim, I.J.; Ramalingam, M.; Son, Y.-A. Investigation of reversible self-thermochromism in microencapsulated fluoran-based materials. *Dye. Pigment.* **2018**, *151*, 64–74. [CrossRef]
26. Panák, O.; Držková, M.; Kaplanová, M.; Novak, U.; Klanjšek Gunde, M. The relation between color and structural changes in thermochromic systems comprising crystal violet lactone, bisphenol A, and tetradecanol. *Dye. Pigment.* **2017**, *136*, 382–389. [CrossRef]
27. Pu, Y.; Fang, J. Preparation and thermochromic behavior of low-temperature thermochromic microcapsule temperature indicators. *Colloids Surf. A Physicochem. Eng. Asp.* **2022**, *653*, 129889. [CrossRef]
28. Hao, P.; Li, H.; Yu, T.; Fu, Y. Pyrazinium iodoargentate with versatile photo- and thermo-chromism. *Dye. Pigment.* **2017**, *136*, 825–829. [CrossRef]
29. Ahn, K.-S.; Lee, D.K.; Kim, J.H.; Kim, S.H. Domino-like thermal phase transition of 2,3-bis(phenylethenyl)-5,6-dicyanopyrazine crystal. *Dye. Pigment.* **2011**, *89*, 93–95. [CrossRef]
30. Liu, Y.; Liu, X.; Tian, Y.; Ran, R.; Du, C.; Wang, Y.; Ma, N.; Li, R.; Chai, X.; Dong, X.; et al. An AIE-active Schiff base derivative with reversible thermochromism based on two-step isomerization in the solid state. *Mater. Today Chem.* **2024**, *40*, 102241. [CrossRef]
31. Wu, H.; Wu, W.; Hu, L.; Zhu, J.; Li, Q.; Gao, Y.; Wei, Y.; Jiang, G.; Yang, Y. Time-resolved encryption from a spiropyran derivative: High-contrasted and multi-state mechanochromism, photochromism and thermochromism. *Chem. Eng. J.* **2023**, *469*, 143781. [CrossRef]
32. Li, C.; Zhang, Y.; Zou, W. Reuse analysis of liquid waste from a thermochromic poplar-based crystal violet lactone/calcium chloride/n-octadecanol/n-dodecanol composite. *Ind. Crops Prod.* **2025**, *224*, 120389. [CrossRef]
33. Arulprakasajothi, M.; Susanth, B.; Naveen Kumar, K.; Madan Mohan Reddy, A. Thermal management on external surfaces by thermochromic materials. *Mater. Today Proc.* **2021**, *47*, 4666–4670. [CrossRef]
34. Zhang, Z.; Liu, Y.; Yang, K.; Chen, D.; Li, S.; Li, Z. Reversible thermochromic microencapsulated phase change materials for enhancing functionality of silicone rubber materials. *Mater. Chem. Phys.* **2022**, *290*, 126564. [CrossRef]
35. Soofivand, F.; Salavati-Niasari, M. "Ag_2HgI_4" a thermochromic compound with superionic conducting properties: Synthesis, characterization and investigation of graphene-based nanocomposites. *J. Mol. Liq.* **2018**, *252*, 112–120. [CrossRef]
36. Cao, Y.; Wang, Y.; Zhang, Y.; Liu, X.; Lin, J. Stable and rapid thermochromic reversibility in acene alkylamine intercalated layered hybrid perovskites. *Mater. Today Commun.* **2023**, *37*, 107544. [CrossRef]
37. Luo, L.; Le Pierrès, N. Innovative Systems for Storage of Thermal Solar Energy in Buildings. In *Solar Energy Storage*; Elsevier: Amsterdam, The Netherlands, 2015; pp. 27–62.
38. Toupka, A.A.; Roussin, L.F.; Patrice, K.T.; Hypolite Mathias, T.K.; Zema, M.; Aquilanti, G.; Tarantino, S.C.; Ignas, T.K.; John, L.N. Fe-doped diaquabis[malonato(1-)-κ^2O,O′]zinc(II) an evidence case of the synthesis of thermochromic materials by metal doping. *Inorganica Chim. Acta* **2025**, *582*, 122677. [CrossRef]
39. Halder, A.; Choudhury, D.; Ghosh, S.; Subbiah, A.S.; Sarkar, S.K. Exploring Thermochromic Behavior of Hydrated Hybrid Perovskites in Solar Cells. *J. Phys. Chem. Lett.* **2015**, *6*, 3180–3184. [CrossRef]

40. Tian, X.; Xu, S.; Wen, J.; Zhu, L.; Ji, C.; Huang, Z.; Wang, X.; Luo, F.; Liu, X.; Lu, Y.; et al. Thermochromic Pr^{3+} doped $CaMoO_4$ phosphor with diverse thermal responses for temperature sensing. *Ceram. Int.* **2023**, *49*, 27126–27137. [CrossRef]
41. Zhang, X.; Wang, S.; Li, W.; Hu, J.; Liu, P.; Zhang, J.; Zhang, Z.; Ivasishin, O.M.; Yuan, L. Pyrochlore structure β-$Bi_2Sn_2O_7$ as reversible thermochromic pigments. *Mater. Lett.* **2023**, *342*, 134319. [CrossRef]
42. Nguyen, D.K.; Lee, H.; Kim, I.-T. Synthesis and thermochromic properties of Cr-doped Al_2O_3 for a reversible thermochromic sensor. *Materials* **2017**, *10*, 476. [CrossRef]
43. Xie, M.; Zhang, Z.; Zhao, Y.; Yu, M.; Jiang, F.; Chen, L.; Hong, M. A copper(I) thiolate coordination polymer with thermochromic and mechanochromic luminescence. *Inorg. Chem. Commun.* **2022**, *140*, 109432. [CrossRef]
44. Tatíčková, Z.; Kudláček, J.; Zoubek, M.; Kuchař, J. Behavior of Thermochromic Coatings under Thermal Exposure. *Coatings* **2023**, *13*, 642. [CrossRef]
45. Garshasbi, S.; Santamouris, M. Using advanced thermochromic technologies in the built environment: Recent development and potential to decrease the energy consumption and fight urban overheating. *Sol. Energy Mater. Sol. Cells* **2019**, *191*, 21–32. [CrossRef]
46. Park, S.-H.; Bae, J. Tailoring environment friendly carbon nanostructures by surfactant mediated interfacial engineering. *J. Ind. Eng. Chem.* **2015**, *30*, 1–9. [CrossRef]
47. Du, Z.; Li, M.; Zou, F.; Song, Y.; Xu, S.; Wu, L.; Li, L.; Li, G. VO_2@SiO_2 Nanoparticle-Based Films with Localized Surface Plasmon Resonance for Smart Windows. *ACS Appl. Nano Mater.* **2022**, *5*, 12972–12979. [CrossRef]
48. Seeboth, A.; Ruhmann, R.; Mühling, O. Thermotropic and Thermochromic Polymer Based Materials for Adaptive Solar Control. *Materials* **2010**, *3*, 5143–5168. [CrossRef]
49. Cao, D.; Xu, C.; Lu, W.; Qin, C.; Cheng, S. Sunlight-Driven Photo-Thermochromic Smart Windows (Solar RRL 4/2018). *Sol. RRL* **2018**, *2*, 1870163. [CrossRef]
50. Shang, L.; Gu, Z.; Zhao, Y. Structural color materials in evolution. *Mater. Today* **2016**, *19*, 420–421. [CrossRef]
51. Fenzl, C.; Hirsch, T.; Wolfbeis, O.S. Photonic Crystals for Chemical Sensing and Biosensing. *Angew. Chem. Int. Ed.* **2014**, *53*, 3318–3335. [CrossRef]
52. Chen, Y.; Zheng, C. Physically Cross-Linked Hydrogel Designed for Thermochromic Smart Windows: Balance between Thermal Stability and Processability. *ACS Sustain. Chem. Eng.* **2025**, *13*, 2574–2585. [CrossRef]
53. Zhang, J.; Zhang, Y.; Yang, J.; Wang, X. Beyond Color Boundaries: Pioneering Developments in Cholesteric Liquid Crystal Photonic Actuators. *Micromachines* **2024**, *15*, 808. [CrossRef]
54. Turvey, M.; Trushkevych, O.; McKnight, D.J.; Edwards, R.S. Ultrasonic displacement measurements from local absorption of ultrasound in thermochromic liquid crystal sensors. *Ultrasonics* **2024**, *141*, 107352. [CrossRef]
55. Warwick, M.E.A.; Dunnill, C.W.; Goodall, J.; Darr, J.A.; Binions, R. Hybrid chemical vapor and nanoceramic aerosol assisted deposition for multifunctional nanocomposite thin films. *Thin Solid Film.* **2011**, *519*, 5942–5948. [CrossRef]
56. Louloudakis, D.; Vernardou, D.; Spanakis, E.; Katsarakis, N.; Koudoumas, E. Thermochromic Vanadium Oxide Coatings Grown by APCVD at Low Temperatures. *Phys. Procedia* **2013**, *46*, 137–141. [CrossRef]
57. Warwick, M.E.A.; Ridley, I.; Binions, R. Thermochromic vanadium dioxide thin films prepared by electric field assisted atmospheric pressure chemical vapor deposition for intelligent glazing application and their energy demand reduction properties. *Sol. Energy Mater. Sol. Cells* **2016**, *157*, 686–694. [CrossRef]
58. Feng, P.; Wang, W.; Wang, K.; Cheng, S.; Jiang, K. synthesized by a facile solid-phase method assisted with agarose as a high-performance cathode for sodium-ion batteries. *J. Mater. Chem. A* **2017**, *5*, 10261–10268. [CrossRef]
59. Zhao, Z.; Chen, Z.; Liu, Y.; Wang, Y.; Xu, M.; Wang, N.; Zhou, Y.; Long, Y. Sn-W Co-Doping Improves Thermochromic Performance of VO_2 Films for Smart Windows. *ACS Appl. Energy Mater.* **2020**, *3*, 9972–9979. [CrossRef]
60. Zhang, L.; Zhu, T.; Xia, F.; Cui, Y.; Xia, H.; Yang, G.; Gao, Y. In situ thermal, optical, and structural investigations on reversible thermochromism in bismuth molybdate. *Ceram. Int.* **2021**, *47*, 25854–25862. [CrossRef]
61. Bai, J.; Zhang, J.; Zhang, B.; Zhang, X.; Cao, Y.; Wang, Y.; Yu, H.; Chen, B. Multiple functions material of Pr^{3+} mono-doped $Mg_3Gd_2Ge_3O_{12}$ for temperature sensing and anti-counterfeiting. *Ceram. Int.* **2025**, *51*, 58756–58763. [CrossRef]
62. Zhao, J.; Zhang, Y.; Wang, T.; Guan, L.; Dong, G.; Liu, Z.; Fu, N.; Wang, F.; Li, X. Preparation and luminescent modulation of $KGaSiO_4$:Eu^{3+} phosphors using for multiple anti-counterfeiting. *Ceram. Int.* **2023**, *49*, 29505–29511. [CrossRef]
63. Ji, H.; Liu, D.; Cheng, H.; Zhang, C.; Yang, L.; Ren, D. Infrared thermochromic properties of monoclinic VO_2 nanopowders using a malic acid-assisted hydrothermal method for adaptive camouflage. *RSC Adv.* **2017**, *7*, 5189–5194. [CrossRef]
64. Wu, J.; Huang, W.; Shi, Q.; Cai, J.; Zhao, D.; Zhang, Y.; Yan, J. Effect of annealing temperature on thermochromic properties of vanadium dioxide thin films deposited by organic sol–gel method. *Appl. Surf. Sci.* **2013**, *268*, 556–560. [CrossRef]
65. Li, D.; Huang, F.; Ding, S. Sol–gel preparation and characterization of nanoporous ZnO/SiO_2 coatings with broadband antireflection properties. *Appl. Surf. Sci.* **2011**, *257*, 9752–9756. [CrossRef]
66. Arjun, N.; Yang, T.C.K.; Pan, G.-T.; Yang, Y.-L.; Kareiva, A. The study of thermochromic and thermo-optical properties of sol–gel V_{1-x-y} WxSiyO_2 films by response surface method. *J. Taiwan Inst. Chem. Eng.* **2016**, *69*, 151–155. [CrossRef]

67. Liang, Z.; Zhao, L.; Meng, W.; Zhong, C.; Wei, S.; Dong, B.; Xu, Z.; Wan, L.; Wang, S. Tungsten-doped vanadium dioxide thin films as smart windows with self-cleaning and energy-saving functions. *J. Alloys Compd.* **2017**, *694*, 124–131. [CrossRef]
68. Lan, S.-D.; Cheng, C.-C.; Huang, C.-H.; Chen, J.-K. Synthesis of sub-10 nm VO_2 nanoparticles films with plasma-treated glass slides by aqueous sol–gel method. *Appl. Surf. Sci.* **2015**, *357*, 2069–2076. [CrossRef]
69. Salamati, M.; Kamyabjou, G.; Mohamadi, M.; Taghizade, K.; Kowsari, E. Preparation of TiO_2@W-VO_2 thermochromic thin film for the application of energy efficient smart windows and energy modeling studies of the produced glass. *Constr. Build. Mater.* **2019**, *218*, 477–482. [CrossRef]
70. Babar, B.M.; Mohite, A.A.; Patil, V.L.; Pawar, U.T.; Kadam, L.D.; Kadam, P.M.; Patil, P.S. Sol-gel prepared vanadium oxide for photocatalytic degradation of Methylene Blue dye. *Mater. Today Proc.* **2021**, *43*, 2673–2677. [CrossRef]
71. Li, P.; Wang, J.; Li, Z.; Zhang, P.; Cao, X.; Xu, J.; Zheng, J.; Lu, Y.; He, Y. Enhancing thermochromic properties of VO_2 amorphous films on glass substrates by Sn-W co-doping. *Infrared Phys. Technol.* **2023**, *134*, 104871. [CrossRef]
72. Yang, G.; Park, S.-J. Conventional and Microwave Hydrothermal Synthesis and Application of Functional Materials: A Review. *Materials* **2019**, *12*, 1177. [CrossRef] [PubMed]
73. Wen, C.; Feng, L.; Li, Z.; Bai, J.; Wang, S.; Gao, X.; Wang, J.; Yao, W. A review of the preparation, properties and applications of VO_2 thin films with the reversible phase transition. *Front. Mater.* **2024**, *11*, 1341518. [CrossRef]
74. Wu, L.; Teng, A.; Li, M.; Li, L.; Huang, Z.; Li, X.; Yu, J.; Xu, S.; Zou, F.; Zou, A.; et al. Kirkendall effect induced ultrafine VOOH nanoparticles and their transformation into VO_2(M) for energy-efficient smart windows. *Mater. Horiz.* **2024**, *11*, 1098–1107. [CrossRef]
75. Zhang, Y.; Li, W.; Fan, M.; Zhang, F.; Zhang, J.; Liu, X.; Zhang, H.; Huang, C.; Li, H. Preparation of W- and Mo-doped VO_2(M) by ethanol reduction of peroxovanadium complexes and their phase transition and optical switching properties. *J. Alloys Compd.* **2012**, *544*, 30–36. [CrossRef]
76. Li, W.; Ji, S.; Qian, K.; Jin, P. Preparation and characterization of VO_2(M)–SnO_2 thermochromic films for application as energy-saving smart coatings. *J. Colloid Interface Sci.* **2015**, *456*, 166–173. [CrossRef]
77. Chen, Y.; Ji, H.; Lu, M.; Liu, B.; Zhao, Y.; Ou, Y.; Wang, Y.; Tao, J.; Zou, T.; Huang, Y.; et al. Machine learning guided hydrothermal synthesis of thermochromic VO_2 nanoparticles. *Ceram. Int.* **2023**, *49*, 30794–30800. [CrossRef]
78. Wang, N.; Goh, Q.S.; Lee, P.L.; Magdassi, S.; Long, Y. One-step hydrothermal synthesis of rare earth/W-codoped VO_2 nanoparticles: Reduced phase transition temperature and improved thermochromic properties. *J. Alloys Compd.* **2017**, *711*, 222–228. [CrossRef]
79. Zhou, Q.; Lv, W.; Qiu, Q.; Zhou, T.; Huang, C.; Li, L. Boron doped M-phase VO_2 nanoparticles with low metal-insulator phase transition temperature for smart windows. *Ceram. Int.* **2020**, *46*, 4786–4794. [CrossRef]
80. Okada, M.; Kuno, M.; Yamada, Y. Fast synthesis of monoclinic VO_2 nanoparticles by microwave-assisted hydrothermal method and application to high-performance thermochromic film. *Sol. Energy Mater. Sol. Cells* **2023**, *255*, 112311. [CrossRef]
81. Marcílio de Souza, A.; Cercena, R.; da Costa Duarte, R.; Arcaro, S.; Dal Bó, A.G. The influence of precursors and additives on the hydrothermal synthesis of VO_2: A route for tuning the metal–insulator transition temperature. *Ceram. Int.* **2020**, *46*, 23560–23566. [CrossRef]
82. Becker, M.; Wollenweber-Bienerth, Y.R.; Hartmann, S.; Polity, A.; Chatterjee, S.; Klar, P.J. Optimization and Validation of the Thermochromic Performance of a Trilayer Coating of TiO_2/VO_2/TiO_2 for Smart Windows. *ACS Appl. Electron. Mater.* **2025**, *7*, 7668–7678. [CrossRef]
83. Powell, M.J.; Quesada-Cabrera, R.; Taylor, A.; Teixeira, D.; Knapp, C.E.; Carmalt, C.J.; Parkin, I.P. Optimized Atmospheric-Pressure Chemical Vapor Deposition Thermochromic VO_2 Thin Films for Intelligent Window Applications. *ACS Omega* **2017**, *2*, 7666–7677. [CrossRef]
84. Liu, C.; Wang, J.-H.; Weng, J. Growth of micro- and nanocrystalline dual layer composite diamond films by microwave plasma CVD: Influence of CO_2 concentration on growth of nano-layer. *J. Cryst. Growth* **2015**, *410*, 30–34. [CrossRef]
85. Warwick, M.E.A.; Binions, R. Chemical vapor deposition of thermochromic vanadium dioxide thin films for energy efficient glazing. *J. Solid State Chem.* **2014**, *214*, 53–66. [CrossRef]
86. Wilkinson, M.; Kafizas, A.; Bawaked, S.M.; Obaid, A.Y.; Al-Thabaiti, S.A.; Basahel, S.N.; Carmalt, C.J.; Parkin, I.P. Combinatorial Atmospheric Pressure Chemical Vapor Deposition of Graded TiO_2–VO_2 Mixed-Phase Composites and Their Dual Functional Property as Self-Cleaning and Photochromic Window Coatings. *ACS Comb. Sci.* **2013**, *15*, 309–319. [CrossRef] [PubMed]
87. Matamura, Y.; Ikenoue, T.; Miyake, M.; Hirato, T. Mist CVD of vanadium dioxide thin films with excellent thermochromic properties using a water-based precursor solution. *Sol. Energy Mater. Sol. Cells* **2021**, *230*, 111287. [CrossRef]
88. Kano, T.; Nishinaka, H.; Arata, Y.; Yoshimoto, M. Nitrogen Doping in VO_2 Thin Films on Synthetic Mica Substrates Through Mist Chemical Vapor Deposition: Lowering the Metal–Insulator Transition Temperature Toward Smart Windows. *Adv. Mater. Interfaces* **2024**, *11*, 2400038. [CrossRef]

89. Du, Y.; Liu, S.; Zhou, Z.; Lee, H.H.; Ho, T.C.; Feng, S.-P.; Tso, C.Y. Study on the halide effect of $MA_4PbX_6 \cdot 2H_2O$ hybrid perovskites–From thermochromic properties to practical deployment for smart windows. *Mater. Today Phys.* **2022**, *23*, 100624. [CrossRef]
90. Top, I.; Binions, R.; Warwick, M.E.A.; Dunnill, C.W.; Holdynski, M.; Abrahams, I. VO_2/TiO_2bilayer films for energy efficient windows with multifunctional properties. *J. Mater. Chem. C* **2018**, *6*, 4485–4493. [CrossRef]
91. Bagochus, E.K.; Mutilin, S.V.; Kichay, V.N.; Yakovkina, L.V. Selective growth of vanadium dioxide on patterned Al/SiO_2 substrates by metal–organic chemical vapor deposition. *CrystEngComm* **2024**, *26*, 4995–5003. [CrossRef]
92. Wu, M.; Zhou, X.; Liang, X.; Han, Y.; Li, Y.; Jiang, X.; Wang, X.; Chai, Y.; Zhou, X.; Yang, H.; et al. $Sn_2P_2S_6$: A lead-free reversible thermochromic ferroelectric with high near-infrared reflectance. *Chem. Eng. J.* **2023**, *452*, 139599. [CrossRef]
93. Paprota, N.; Szumera, M.; Pielichowska, K. The Impact of Boron Nitride Additive on Thermal and Thermochromic Properties of Organic Thermochromic Phase Change Materials. *Materials* **2024**, *17*, 3632. [CrossRef] [PubMed]
94. Grave, D.A.; Schmitt, M.P.; Robinson, J.A.; Wolfe, D.E. Stress induced phase transition in Gd_2O_3 films by ion beam assisted reactive electron beam-physical vapor deposition (EB-PVD). *Surf. Coat. Technol.* **2014**, *242*, 68–73. [CrossRef]
95. Lafort, A.; Kebaili, H.; Goumri-Said, S.; Deparis, O.; Cloots, R.; De Coninck, J.; Voué, M.; Mirabella, F.; Maseri, F.; Lucas, S. Optical properties of thermochromic VO_2 thin films on stainless steel: Experimental and theoretical studies. *Thin Solid Film.* **2011**, *519*, 3283–3287. [CrossRef]
96. Gonçalves, A.; Resende, J.; Marques, A.C.; Pinto, J.V.; Nunes, D.; Marie, A.; Goncalves, R.; Pereira, L.; Martins, R.; Fortunato, E. Smart optically active VO_2 nanostructured layers applied in roof-type ceramic tiles for energy efficiency. *Sol. Energy Mater. Sol. Cells* **2016**, *150*, 1–9. [CrossRef]
97. Liubchenko, O.; Kladko, V.; Melnik, V.; Romanyuk, B.; Gudymenko, O.; Sabov, T.; Dubikovskyi, O.; Maksimenko, Z.; Kosulya, O.; Kulbachynskyi, O. Ar-implanted vanadium dioxide thin film with the reduced phase transition temperature. *Mater. Lett.* **2022**, *314*, 131895. [CrossRef]
98. Zhu, M.; Zhang, D.; Qi, H. The novel preparation method of thermochromic VO_2 films with a low phase transition temperature by thermal oxidation of V–Mo cosputtered alloy films. *Ceram. Int.* **2023**, *49*, 11803–11812. [CrossRef]
99. Santos, A.J.; Martin, N.; Outón, J.; Blanco, E.; García, R.; Morales, F.M. Towards the optimization of a simple route for the fabrication of energy-efficient VO_2-based smart coatings. *Sol. Energy Mater. Sol. Cells* **2023**, *254*, 112253. [CrossRef]
100. Jin, W.; Park, K.; Cho, J.Y.; Bae, S.-H.; Siyar, M.; Jang, H.; Park, C. Thermochromic properties of ZnO/VO_2ZnO films on soda lime silicate glass deposited by RF magnetron sputtering. *Ceram. Int.* **2023**, *49*, 10437–10444. [CrossRef]
101. Zong, H.; Zhang, S.; Bian, L.; Chen, H.; Liu, Z.; Sun, B.; Qiao, W.; Yan, L.; Hu, Q.; Li, M. Preparation and characterization of VO_2/Cu-Zr NPs/VO_2 composite films with enhanced thermochromic properties. *J. Alloys Compd.* **2023**, *967*, 171654. [CrossRef]
102. Cezar, A.B.; Graff, I.L.; Rikers, Y.; Schreiner, W.H.; Mattoso, N. Highly Oriented VO_2 Thin Films Prepared by Electrodeposition. *Electrochem. Solid-State Lett.* **2011**, *14*, D23. [CrossRef]
103. Koza, J.A.; He, Z.; Miller, A.S.; Switzer, J.A. Resistance Switching in Electrodeposited VO_2 Thin Films. *Chem. Mater.* **2011**, *23*, 4105–4108. [CrossRef]
104. Tominaga, T.; Mochida, T. Multifunctional Ionic Liquids from Rhodium(I) Isocyanide Complexes: Thermochromic, Fluorescence, and Chemochromic Properties Based on Rh−Rh Interaction and Oxidative Addition. *Chem.–A Eur. J.* **2018**, *24*, 6239–6247. [CrossRef] [PubMed]
105. Lai, X.; Li, Y.; Yang, Y.; Zhou, Z.; Wang, C. Vanadium dioxide (IV) (B) nanostructures prepared via electrodeposition for zinc-ion storage in electrochemical energy storage devices. *J. Energy Storage* **2024**, *102*, 114157. [CrossRef]
106. Liu, H.; Jiao, L.; Lin, H.; Li, L. Design and application research of portable reversible thermochromic patches in grid power supply systems. *AIP Adv.* **2024**, *14*, 045322. [CrossRef]
107. Du, J.; Gao, Y.; Luo, H.; Kang, L.; Zhang, Z.; Chen, Z.; Cao, C. Significant changes in phase-transition hysteresis for Ti-doped VO_2 films prepared by polymer-assisted deposition. *Sol. Energy Mater. Sol. Cells* **2011**, *95*, 469–475. [CrossRef]
108. Gao, M.; Wang, X.; Luo, S.; Lu, Q.; Luo, S.-N.; Lu, C.; Chen, S.; Long, F.; Lin, Y. Terahertz transmission properties of vanadium dioxide films deposited on gold grating structure with different periods. *Mater. Res. Express* **2020**, *7*, 056404. [CrossRef]
109. Yue, F.; Huang, W.; Shi, Q.; Li, D.; Hu, Y.; Xiao, Y.; Deng, X.; Wang, C. Phase transition properties of vanadium oxide films deposited by polymer-assisted deposition. *J. Sol-Gel Sci. Technol.* **2014**, *72*, 565–570. [CrossRef]
110. Morini, E.; Castellani, B.; Nicolini, A.; Rossi, F.; Berardi, U. Effects of aging on retro-reflective materials for building applications. *Energy Build.* **2018**, *179*, 121–132. [CrossRef]
111. Guo, H.; Yuan, L.; Wang, S.; Hou, C. Tetrahedral coordinated Mn(V) in $Ba_3V_2O_8$ with varied stoichiometry as thermally stable turquoise to dodger blue inorganic pigments. *Ceram. Int.* **2024**, *50*, 3110–3118. [CrossRef]
112. Ma, X.-G.; Wang, L.; Li, L.; Bian, L.-R.; Yang, W.-F.; Meng, Q.-T. The novel thermochromic and energy-storage microcapsules with significant extension of color change range to different tones. *J. Macromol. Sci. A* **2019**, *56*, 588–596. [CrossRef]

113. Li, Y.; Yang, A.; Li, Y.; Jiang, Z.; He, F.; Chen, Z.; Li, X.; Said, Z.; Shehzad, N.; Waqas, A.; et al. TC@MF phase change microcapsules with reversibly thermochromic property for temperature response and thermoregulation. *Colloids Surf. A Physicochem. Eng. Asp.* **2023**, *677*, 132333. [CrossRef]
114. Ji, S.; Wang, M.; Su, C.; Zou, Y.; Gao, J. Preparation and performance of thermochromic solid-solid phase change materials based on negative photochromic spiropyran. *Polymer* **2025**, *318*, 127995. [CrossRef]
115. Geng, C.; Zhang, M.; Wei, H.; Gu, J.; Zhao, T.; Guan, H.; Liang, S.; Boytsova, O.; Dou, S.; Chen, Y.; et al. Tracking the optical constants of self-patterned VO_2-based on smart windows during metal-insulator transition. *Sol. Energy Mater. Sol. Cells* **2024**, *272*, 112892. [CrossRef]
116. Liu, S.; Wang, J.; Meng, X. Influence of thermochromic coatings on the thermal performance of the multi-layer wall by numerical simulation. *Int. J. Low-Carbon Technol.* **2022**, *17*, 1366–1374. [CrossRef]
117. Castellani, B.; Morini, E.; Anderini, E.; Filipponi, M.; Rossi, F. Development and characterization of retro-reflective colored tiles for advanced building skins. *Energy Build.* **2017**, *154*, 513–522. [CrossRef]
118. Wang, X.; Li, M.; Wang, Q.; Zhang, J.; Shi, J.; Lu, Y.; Li, G. Effect of Mie Scattering on Thermochromic Performance of Branched VO_2 Prepared by One-Step Hydrothermal Method. *Eur. J. Inorg. Chem.* **2020**, *2020*, 2872–2878. [CrossRef]
119. Zhang, B.; Luo, J.; Tian, Y.; Liu, S. Preparation and thermochromic properties of Mn-doped ZnO materials. *Ordnance Mater. Sci. Eng.* **2024**, *47*, 51–56.
120. Xi, Y.; Xu, S.; Zhang, J. Reversible thermochromic composites for intelligent adjustment of solar reflectance. *Mater. Chem. Phys.* **2022**, *276*, 125372. [CrossRef]
121. Liu, Y.; Wang, Y.; Zhang, X.; Li, M. A long-term stable thermochromic smart window of PNIPAM-based hydrogels with excellent water retention and visible light modulation. *J. Mater. Chem. A* **2026**, *14*, 10657–10667. [CrossRef]
122. Yan, J.; Zhang, H.; Bai, Y.; Wei, X.; Zheng, X.; She, M.; Cheng, C.; Lei, T.; Ming, R.; Wang, L.; et al. Nature loofah network-inspired rapid thermal-conductive and thermochromic-based nanocomposites for efficient heat management in advanced electronic devices. *Polym. Compos.* **2025**, *46*, 5685–5693. [CrossRef]
123. Li, M.; Zhou, S. Experimental investigation on the thermal performance of the LDHs-based thermochromic temperature control coatings. *Sol. Energy Mater. Sol. Cells* **2026**, *296*, 114068. [CrossRef]
124. Luo, W.; Qin, Y.; Ma, Z.; Wang, L.; Cheng, Q.; Tan, C.; Zhang, M.; Zhang, H.; Wang, B.; Song, X. Exploring the thermochromic properties of fluoran-based complexes: Synthesis, structural influence, and application in temperature sensing. *Dye. Pigment.* **2025**, *232*, 112483. [CrossRef]
125. Zhu, Z.; Zhu, K.; Guo, J.; Fan, Z.; Li, Z.; Zhang, J. Preparation and durability evaluation of vanadium dioxide intelligent thermal insulation films. *Colloid Interface Sci. Commun.* **2022**, *48*, 100619. [CrossRef]
126. Yuan, A.; Zhao, S.; Liu, T.; Zhao, Y.; Jiang, L.; Lei, J. Temperature-Responsive Thermochromic Phase Change Materials with Tunable Photothermal Conversion Efficiency Toward Solar Energy Storage. *Adv. Mater. Technol.* **2022**, *7*, 2200226. [CrossRef]
127. Zhou, Y.; Zhao, S.; Qi, S.; Liu, Y.; Chen, N.; Wang, L.; Niu, Y.; Xu, Q. VO_2 Nanoparticles-Based Thermochromic Smart Windows. *ChemistrySelect* **2023**, *8*, e202302259. [CrossRef]
128. Chocolatl-Torres, M.; Franco-Bacca, A.P.; Ramírez-Rincón, J.A.; Gómez-Heredia, C.L.; Cervantes-Alvarez, F.; Alvarado-Gil, J.J.; Silva-Gonzalez, R.; Toledo, M.; Salazar-Kuri, U. Study of structural and optical properties of the thermochromic silver and copper tetraiodomercurates (Ag_2, Cu_2) HgI_4 ceramics. *Appl. Phys. A* **2020**, *126*, 525. [CrossRef]
129. Nguyen, D.K.; Bach, Q.-V.; Kim, B.; Lee, H.; Kim, I.-T. Synthesis of Cr-doped Al_2O_3 by Pechini sol-gel method and its application for reversible thermochromic sensors. *Mater. Chem. Phys.* **2019**, *223*, 708–714. [CrossRef]
130. Ge, Y.; Shah, Z.H.; Wang, C.; Wang, J.; Mao, W.; Zhang, S.; Lu, R. In situ encapsulation of ultrasmall CuO quantum dots with controlled band-gap and reversible thermochromism. *ACS Appl. Mater. Interfaces* **2015**, *7*, 26437–26444. [CrossRef] [PubMed]
131. Xie, D.; Xu, J.; Cheng, H.; Wang, N.; Zhou, Q. The role played by amine and ethyl group in the reversible thermochromic process of $[(C_2H_5)_2NH_2]_2CuCl_4$ probing by FTIR and 2D-COS analysis. *J. Mol. Struct.* **2018**, *1161*, 267–272. [CrossRef]
132. Zhang, B.; Xu, C.; Xu, G.; Xiang, S.; Zhu, Y. Thermochromic and infrared emissivity characteristics of cobalt doped zinc oxide for smart stealth in visible-infrared region. *Opt. Mater.* **2018**, *86*, 464–470. [CrossRef]
133. Boontan, S.; Boonkham, S.; Soltani, M.T.; Chae, M.; Ryu, S.; Lee, G.H.; Phatanasri, S.; Cho, J. Stabilization of the VO_2(M2) Phase and Change in Lattice Parameters at the Phase Transition Temperature of $W_XV_{1-X}O_2$ Thin Films. *ACS Appl. Mater. Interfaces* **2023**, *15*, 51433–51445. [CrossRef] [PubMed]
134. Zhou, Y.; Duan, R. Leak-Proof Reversible Thermochromic Microcapsule Phase Change Materials with High Latent Thermal Storage for Thermal Management. *ACS Appl. Energy Mater.* **2024**, *7*, 5944–5956. [CrossRef]
135. Kumari, R.; De, A.; Bhattacharyya, A.J.; Row, T.N.G. Designing multifunctional organic thermochromic ferroelectric materials: Remarkable melt-cool large thermal hysteresis of reversible single crystal to single crystal transformation. *Mater. Adv.* **2024**, *5*, 3411–3423. [CrossRef]
136. Wu, Z.; Zhang, W.; Han, N.; Zhang, X.; Li, W. Reversible Thermochromic Nanofiber Membrane for Energy Storage and Thermoregulation. *ACS Appl. Energy Mater.* **2023**, *6*, 2423–2433. [CrossRef]

137. Li, M.; Zhou, S. Discoloration performance and mechanism research of a novel thermochromic energy storage material. *Renew. Energy* **2024**, *225*, 120340. [CrossRef]
138. Kumar, S.; Qadir, A.; Maury, F.; Bahlawane, N. Visible Thermochromism in Vanadium Pentoxide Coatings. *ACS Appl. Mater. Interfaces* **2017**, *9*, 21447–21456. [CrossRef]
139. Long, L.; Ye, H. Discussion of the performance improvement of thermochromic smart glazing applied in passive buildings. *Sol. Energy* **2014**, *107*, 236–244. [CrossRef]
140. Tong, K.; Li, R.; Zhu, J.; Yao, H.; Zhou, H.; Zeng, X.; Ji, S.; Jin, P. Preparation of VO_2/Al-O core-shell structure with enhanced weathering resistance for smart window. *Ceram. Int.* **2017**, *43*, 4055–4061. [CrossRef]
141. Gao, Y.; Wang, S.; Luo, H.; Dai, L.; Cao, C.; Liu, Y.; Chen, Z.; Kanehira, M. Enhanced chemical stability of VO_2 nanoparticles by the formation of SiO_2/VO_2 core/shell structures and the application to transparent and flexible VO_2-based composite foils with excellent thermochromic properties for solar heat control. *Energy Environ. Sci.* **2012**, *5*, 6104–6110. [CrossRef]
142. Li, Y.; Ji, S.; Gao, Y.; Luo, H.; Kanehira, M. Core-shell VO_2@TiO_2 nanorods that combine thermochromic and photocatalytic properties for application as energy-saving smart coatings. *Sci. Rep.* **2013**, *3*, 1370. [CrossRef]
143. Chen, Y.; Zeng, X.; Zhu, J.; Li, R.; Yao, H.; Cao, X.; Ji, S.; Jin, P. High Performance and Enhanced Durability of Thermochromic Films Using VO_2@ZnO Core–Shell Nanoparticles. *ACS Appl. Mater. Interfaces* **2017**, *9*, 27784–27791. [CrossRef]
144. Zhao, X.; Sun, J.; Ma, J.; Liu, T.; Guo, Z.; Yang, Z.; Yao, W.; Jiang, X. Combining reversible addition-fragmentation chain transfer polymerization and thiol-ene click reaction for application of core-shell structured VO_2@polymer nanoparticles to smart window. *Sustain. Mater. Technol.* **2022**, *32*, e00420. [CrossRef]
145. Saini, M.; Dehiya, B.S.; Umar, A. VO_2 (M)@CeO2 core-shell nanospheres for thermochromic smart windows and photocatalytic applications. *Ceram. Int.* **2020**, *46*, 986–995. [CrossRef]
146. Li, D.; Deng, S.; Zhao, Z.; Yang, J.; Wang, B.; Li, J.; Jin, H. VO_2(M)@SnO_2 core–shell nanoparticles: Improved chemical stability and thermochromic property rendered by SnO_2 shell. *Appl. Surf. Sci.* **2022**, *598*, 153741. [CrossRef]
147. Liang, J.; Zhang, C.; Yu, Y.; Bai, Y.; Yang, G.; Zhang, D.; Lei, D. Thermochromic performance improvement based on W-VO_2@AA core-shell structure nanoparticles. *Opt. Mater.* **2025**, *165*, 117126. [CrossRef]
148. Zheng, J.; Wang, S.; Ke, Y. Recent developments in nanostructured vanadium dioxide films for smart windows. *Nanoscale* **2021**, *13*, 14594–14611.
149. Zou, Z.; Zhang, Z.; Xu, J.; Li, G.; Xiong, R.; Liu, Y.; Shi, J. Phase transition mechanism and application of silicon-doped VO_2 thin films to smart windows. *J. Mater. Sci. Mater. Electron.* **2021**, *32*, 23825–23833. [CrossRef]
150. Guo, H.; Wang, Y.G.; Fu, H.R.; Jain, A.; Chen, F.G. Influence of dopant valence on the thermochromic properties of VO_2 nanoparticles. *Ceram. Int.* **2021**, *47*, 21873–21881. [CrossRef]
151. Zhou, D.; Zong, H.; Hu, Q.; Yan, L.; Qiao, W.; Zhang, S.; Pan, J.; Liu, Z.; Li, M. Symmetrical SnO_2/W-doped VO_2/SnO_2 sandwich structures with high luminous transmittance, excellent solar modulation ability and low phase transition temperature. *Infrared Phys. Technol.* **2022**, *123*, 104198. [CrossRef]
152. Rezek, J.; Szelwicka, J.; Vlček, J.; Čerstvý, R.; Houška, J.; Fahland, M.; Fahlteich, J. Transfer of the sputter technique for deposition of strongly thermochromic VO_2-based coatings on ultrathin flexible glass to large-scale roll-to-roll device. *Surf. Coat. Technol.* **2022**, *442*, 128273. [CrossRef]
153. Cui, Y.; Shi, S.; Chen, L.; Luo, H.; Gao, Y. Hydrogen-doping induced reduction in the phase transition temperature of VO_2: A first-principles study. *Phys. Chem. Chem. Phys.* **2015**, *17*, 20998–21004. [CrossRef]
154. Haji, H.F.; Numan, N.; Madiba, I.G.; Samiji, M.E.; Mlyuka, N.R.; Maaza, M. Zr and W Co-doped VO_2 Thin Films with Improved Luminous Transmittance and Transition Temperature. *J. Mater. Sci. Mater. Electron.* **2023**, *34*, 2006. [CrossRef]
155. Xu, Q.; Ke, Y.; Feng, C.; Chen, C.; Wen, Z.; Wang, H.; Sun, M.; Liu, X.; Liu, H.; Magdassi, S.; et al. Anisotropic localized surface plasmon resonance of vanadium dioxide rods in flexible thermochromic film towards multifunctionality. *Sol. Energy Mater. Sol. Cells* **2021**, *230*, 111163. [CrossRef]
156. Wang, X.; Chen, L.; Lu, H.; Fang, W.; Li, H.; Yin, W.; Li, M.; Lu, Y.; Li, P.; He, Y. Enhancing visible-light transmittance while reducing phase transition temperature of VO_2 by Hf–W co-doping. *Appl. Phys. Lett.* **2021**, *118*, 192102. [CrossRef]
157. Zhao, L.; Miao, L.; Liu, C.; Li, C.; Asaka, T.; Kang, Y.; Iwamoto, Y.; Tanemura, S.; Gu, H.; Su, H. Solution-processed VO_2-SiO_2 composite films with simultaneously enhanced luminous transmittance, solar modulation ability and anti-oxidation property. *Sci. Rep.* **2014**, *4*, 7000. [CrossRef] [PubMed]
158. Chen, Z.; Gao, Y.; Kang, L.; Du, J.; Zhang, Z.; Luo, H.; Miao, H.; Tan, G. VO_2-based double-layered films for smart windows: Optical design, all-solution preparation and improved properties. *Sol. Energy Mater. Sol. Cells* **2011**, *95*, 2677–2684. [CrossRef]
159. Liu, C.; Wang, S.; Zhou, Y.; Yang, H.; Lu, Q.; Mandler, D.; Magdassi, S.; Tay, C.Y.; Long, Y. Index-tunable anti-reflection coatings: Maximizing solar modulation ability for vanadium dioxide-based smart thermochromic glazing. *J. Alloys Compd.* **2018**, *731*, 1197–1207. [CrossRef]

160. Liu, H.; Zong, H.; Yan, L.; Zhou, D.; Yin, Y.; Cao, G.; Bian, L.; Kang, C.; Li, M. $SnO_2/VO_2/SnO_2$ tri-layer thermochromic films with high luminous transmittance, remarkable solar modulation ability and excellent hydrophobicity grown on glass substrates. *Infrared Phys. Technol.* **2021**, *113*, 103648. [CrossRef]
161. Zong, H.; Zhou, D.; Yan, L.; Li, M.; Qiao, W.; Zhang, S.; Hu, Q.; Bian, L. Preparation and characterization of $HfO_2/VO_2/HfO_2$ sandwich structures with low phase transition temperature, excellent thermochromic properties, and superior durability. *Ceram. Int.* **2022**, *48*, 6734–6744. [CrossRef]
162. Bleu, Y.; Bourquard, F.; Poulet, A.; Misdanitis, K.; Jamon, D.; Loir, A.-S.; Garrelie, F.; Donnet, C. Thermochromic properties of $BN/VO_2/BN$ trilayer films with low phase transition temperature and high hysteresis width. *Ceram. Int.* **2023**, *49*, 13542–13547. [CrossRef]
163. Qin, M.; Wang, J.; Tian, S.; Zhao, X.; Liu, B. Customized designs, preparations, and characterizations of high-performance multilayer VO_2-based thermochromic smart coatings. *J. Appl. Phys.* **2024**, *135*, 075301. [CrossRef]
164. Zhan, Y.; Lu, Y.; Xiao, X.; Wang, J.; Liu, Y.; Zhang, S.; Shen, C.; Xu, X.; Xu, G. Tuning thermochromic performance of VOx-based multilayer films by controlling annealing pressure. *Ceram. Int.* **2020**, *46*, 2079–2085. [CrossRef]
165. Long, S.; Cao, X.; Li, N.; Xin, Y.; Sun, G.; Chang, T.; Bao, S.; Jin, P. Application-oriented VO_2 thermochromic coatings with composite structures: Optimized optical performance and robust fatigue properties. *Sol. Energy Mater. Sol. Cells* **2019**, *189*, 138–148. [CrossRef]
166. Yao, L.; Qu, Z.; Sun, R.; Pang, Z.; Wang, Y.; Jin, B.; He, J. Long-Lived Multilayer Coatings for Smart Windows: Integration of Energy-Saving, Antifogging, and Self-Healing Functions. *ACS Appl. Energy Mater.* **2019**, *2*, 7467–7473. [CrossRef]
167. Long, S.; Zhou, H.; Bao, S.; Xin, Y.; Cao, X.; Jin, P. Thermochromic multilayer films of $WO_3/VO_2/WO_3$ sandwich structure with enhanced luminous transmittance and durability. *RSC Adv.* **2016**, *6*, 106435–106442. [CrossRef]
168. Azhan, N.H.; Su, K.; Okimura, K.; Sakai, J. Radio frequency substrate biasing effects on the insulator-metal transition behavior of reactively sputtered VO_2 films on sapphire (001). *J. Appl. Phys.* **2015**, *117*, 185307. [CrossRef]
169. Graf, D.; Schläfer, J.; Garbe, S.; Klein, A.; Mathur, S. Interdependence of structure, morphology, and phase transitions in CVD grown VO_2 and V_2O_3 nanostructures. *Chem. Mater.* **2017**, *29*, 5877–5885. [CrossRef]
170. Wan, M.; Liu, B.; Wang, S.; Hu, L.; He, Y.; Tao, H.; Zhao, X. Optical properties and formation mechanism of M1-phase VO_2 thin films annealed in a closed NH3 atmosphere. *J. Alloys Compd.* **2017**, *706*, 289–296. [CrossRef]
171. Li, M.; Magdassi, S.; Gao, Y.; Long, Y. Hydrothermal synthesis of VO_2 polymorphs: Advantages, challenges and prospects for the application of energy efficient smart windows. *Small* **2017**, *13*, 1701147. [CrossRef]
172. Niu, C.; Meng, J.; Han, C.; Zhao, K.; Yan, M.; Mai, L. VO_2 nanowires assembled into hollow microspheres for high-rate and long-life lithium batteries. *Nano Lett.* **2014**, *14*, 2873–2878. [CrossRef] [PubMed]
173. Zhang, L.; Xia, F.; Song, Z.; Webster, N.A.; Song, J.; Luo, H.; Gao, Y. Phase and morphology evolution during the solvothermal synthesis of VO 2 polymorphs. *Inorg. Chem. Front.* **2016**, *3*, 117–124. [CrossRef]
174. Ayaz, R.M.A.; Balazadeh Koucheh, A.B.; Sendur, K. Broadband-Tunable Vanadium Dioxide (VO_2)-Based Linear Optical Cavity Sensor. *Nanomaterials* **2024**, *14*, 328. [CrossRef] [PubMed]
175. Zhao, X.; Sun, J.; Guo, Z.; Su, J.; Liu, T.; Hu, R.; Yao, W.; Jiang, X. One-step hydrothermal synthesis of monoclinic vanadium dioxide nanoparticles with low phase transition temperature. *Chem. Eng. J.* **2022**, *446*, 137308. [CrossRef]
176. Molloro, L.H.; Tain, S.; Belachew, N.; Owusu, K.A.; Zhao, X. 3D mesoporous structure assembled from monoclinic M-phase VO_2 nanoflakes with enhanced thermochromic performance. *RSC Adv.* **2021**, *11*, 13556–13563. [CrossRef]
177. Zhang, L.; Xia, F.; Yao, J.; Zhu, T.; Xia, H.; Yang, G.; Liu, B.; Gao, Y. Facile synthesis, formation mechanism and thermochromic properties of W-doped VO_2(M) nanoparticles for smart window applications. *J. Mater. Chem. C* **2020**, *8*, 13396–13404. [CrossRef]
178. Wang, S.; Li, C.; Tian, S.; Liu, B.; Zhao, X. Facile synthesis of VO_2(D) and its transformation to VO_2(M) with enhanced thermochromic properties for smart windows. *Ceram. Int.* **2020**, *46*, 14739–14746. [CrossRef]
179. Chang, Q.; Wang, D.; Zhao, Z.; Ling, C.; Wang, C.; Jin, H.; Li, J. Size-Controllable M-Phase VO_2 Nanocrystals for Flexible Thermochromic Energy-Saving Windows. *ACS Appl. Nano Mater.* **2021**, *4*, 6778–6785. [CrossRef]
180. Guo, H.; Wang, Y.G.; Jain, A.; Fu, H.R.; Chen, F.G. Preparation of W/Zr co-doped VO_2 with improved microstructural and thermochromic properties. *J. Alloys Compd.* **2021**, *878*, 160352. [CrossRef]
181. Barinova, S.; Bhupathi, S.; Kazansky, P.G.; Long, Y.; Abdulhalim, I. Smart window based on integration of nanoporous microparticles in liquid crystal composite with metamaterial nanostructured VO_2 film. *J. Photonics Energy* **2024**, *14*, 048001. [CrossRef]
182. Victor, J.L.; Marcel, C.; Sauques, L.; Labrugère, C.; Amiard, F.; Gibaud, A.; Rougier, A. From multilayers to V1-xWxO2$\pm\delta$ films elaborated by magnetron sputtering for decreasing thermochromic transition temperature. *J. Alloys Compd.* **2021**, *858*, 157658. [CrossRef]
183. Savorianakis, G.; Rousseau, C.; Battie, Y.; En Naciri, A.; Maes, B.; Voué, M.; Konstantinidis, S. Optical anisotropy of nanostructured vanadium dioxide thermochromic thin films synthesized by reactive magnetron sputtering combined with glancing angle deposition. *Surf. Coat. Technol.* **2025**, *502*, 131938. [CrossRef]

184. Ho, H.-C.; Lai, Y.-C.; Chen, K.; Dao, T.D.; Hsueh, C.-H.; Nagao, T. High quality thermochromic VO_2 films prepared by magnetron sputtering using V_2O_5 target with in situ annealing. *Appl. Surf. Sci.* **2019**, *495*, 143436. [CrossRef]
185. Zhan, Y.; Xiao, X.; Lu, Y.; Cao, Z.; Qi, S.; Huan, C.; Cheng, H.; Shi, J.; Xu, G. Enhanced thermal stability and thermochromic properties of VOx-based thin films by room-temperature magnetron sputtering. *Sol. Energy Mater. Sol. Cells* **2018**, *174*, 102–111. [CrossRef]
186. Vu, T.D.; Liu, S.; Zeng, X.; Li, C.; Long, Y. High-power impulse magnetron sputtering deposition of high crystallinity vanadium dioxide for thermochromic smart windows applications. *Ceram. Int.* **2020**, *46*, 8145–8153. [CrossRef]
187. Crosby, P.H.; Netravali, A.N. Green thermochromic materials: A brief review. *Adv. Sustain. Syst.* **2022**, *6*, 2200208. [CrossRef]
188. Zhou, J.; Gao, Y.; Zhang, Z.; Luo, H.; Cao, C.; Chen, Z.; Dai, L.; Liu, X. VO_2 thermochromic smart window for energy savings and generation. *Sci. Rep.* **2013**, *3*, 3029. [CrossRef]
189. Xie, G.; Li, Y.; Luo, J.; Wu, C.; Cao, M.; Zhu, D.; Wu, X.; Xie, H.; Yu, W. Scalable Fabrication of Thermochromic Smart Windows for Broadening Temperature Ranges and Their Coupled Thermoelectric Power Generation. *ACS Sustain. Chem. Eng.* **2024**, *12*, 14890–14901. [CrossRef]
190. Yang, C.; He, Y.; Chen, Y.; Li, N. The Effects of Window Geometry Parameters on Indoor Thermal and Visual Comfort of Thermochromic Windows in Office Building. *Buildings* **2025**, *15*, 3963. [CrossRef]
191. Aburas, M.; Soebarto, V.; Williamson, T.; Liang, R.; Ebendorff-Heidepriem, H.; Wu, Y. Thermochromic smart window technologies for building application: A review. *Appl. Energy* **2019**, *255*, 113522. [CrossRef]
192. Zhang, R.; Xiang, B.; Feng, M.; Xia, L.; Xu, L.; Tang, S.; Guan, Q. Energy-Efficient Smart Window Based on Thermochromic Hydrogel with Ultrahigh Visible Transparency and Unprecedented Infrared Transmittance Modulation. *J. Mater. Chem. A* **2021**, *9*, 8712–8724.
193. Tan, X.; Yao, T.; Long, R.; Sun, Z.; Feng, Y.; Cheng, H.; Yuan, X.; Zhang, W.; Liu, Q.; Wu, C. Unraveling metal-insulator transition mechanism of VO_2 triggered by tungsten doping. *Sci. Rep.* **2012**, *2*, 466. [CrossRef]
194. Wang, N.; Duchamp, M.; Xue, C.; Dunin-Borkowski, R.E.; Liu, G.; Long, Y. Single-crystalline W-doped VO_2 nanobeams with highly reversible electrical and plasmonic responses near room temperature. *Adv. Mater. Interfaces* **2016**, *3*, 1600164. [CrossRef]
195. Zong, H.; Tao, X.; Chen, H.; Qiao, W.; Zhang, C.; Li, M.; Yin, Y.; Li, W. Enhanced Thermochromic Performance and Color Display in Au/VO_2 Composite Films Via ZrO_2 Dielectric Interfacial Layers. *Sol. Energy Mater. Sol. Cells* **2025**, *297*, 114104. [CrossRef]
196. Hu, L.; Tao, H.; Chen, G.; Pan, R.; Wan, M.; Xiong, D.; Zhao, X. Porous W-doped VO_2 films with simultaneously enhanced visible transparency and thermochromic properties. *J. Sol-Gel Sci. Technol.* **2016**, *77*, 85–93. [CrossRef]
197. Liu, M.; Su, B.; Kaneti, Y.V.; Chen, Z.; Tang, Y.; Yuan, Y.; Gao, Y.; Jiang, L.; Jiang, X.; Yu, A. Dual-phase transformation: Spontaneous self-template surface-patterning strategy for ultra-transparent VO_2 solar modulating coatings. *ACS Nano* **2017**, *11*, 407–415. [CrossRef]
198. Liu, M.; Su, B.; Tang, Y.; Jiang, X.; Yu, A. Recent advances in nanostructured vanadium oxides and composites for energy conversion. *Adv. Energy Mater.* **2017**, *7*, 1700885. [CrossRef]
199. Chu, X.; Tao, H.; Liu, Y.; Ni, J.; Bao, J.; Zhao, X. VO_2/AZO double-layer films with thermochromism and low-emissivity for smart window applications. *J. Non-Cryst. Solids* **2014**, *383*, 121–125. [CrossRef]
200. Li, X.; Zhou, S.; Wang, Y. Multifunctional VO_2-based smart windows: A review. *J. Alloys Compd.* **2022**, *897*, 163234.
201. Xu, F.; Jin, P.S.; Luo, H.J.; Cao, X. VO_2 Thermochromic Smart Window: Status, Challenges and Prospects. *J. Inorg. Mater.* **2021**, *36*, 1013–1021. [CrossRef]
202. Wu, D.; Su, Q.; Li, Y.; Zhang, C.; Qin, X.; Liu, Y.Y.; Xi, W.S.; Gao, Y.; Cao, A.; Liu, X. Toxicity assessment and mechanistic investigation of engineered monoclinic VO_2 nanoparticles. *Nanoscale* **2018**, *10*, 9736–9746. [CrossRef]
203. Li, J.; Nagamani, C.; Moore, J.S. Polymer mechanochemistry: From destructive to productive. *Acc. Chem. Res.* **2015**, *48*, 2181–2190. [CrossRef]
204. Goyal, S.; Sharma, D.; Sharma, A.L.; Kumar, K. Novel low-temperature colorimetric indicator based on functional PDA/PVA. *Chem. Phys. Impact* **2025**, *10*, 100803. [CrossRef]
205. Park, I.S.; Park, H.J.; Kim, J.-M. A Soluble, Low-Temperature Thermochromic and Chemically Reactive Polydiacetylene. *ACS Appl. Mater. Interfaces* **2013**, *5*, 8805–8812. [CrossRef]
206. Raji, M.; Essabir, H.; Bouhfid, R.; Qaiss, A.e.K. Edible thermochromic beads from flavonoid, fatty acid, and lecithin for smart packaging. *Food Chem.* **2024**, *454*, 139698. [CrossRef]
207. Thomas, J.P.; Amal Raj, R.B.; Virat, G.; Dev, A.V.; Vijayakumar, C.; Gowd, E.B. Proximity-induced FRET and charge-transfer between quantum dots and curcumin enable reversible thermochromic hybrid polymeric films††Electronic supplementary information (ESI) available. *Chem. Commun.* **2024**, *60*, 10954–10957. [CrossRef] [PubMed]
208. Geng, X.; Gao, Y.; Wang, N.; Han, N.; Zhang, X.; Li, W. Intelligent adjustment of light-to-thermal energy conversion efficiency of thermo-regulated fabric containing reversible thermochromic MicroPCMs. *Chem. Eng. J.* **2021**, *408*, 127276. [CrossRef]
209. Liu, Y.; Wu, Y.; Ma, Y.; Wang, P.; Yu, B.; Pei, X.; Liu, S.; Zhou, F. Reversible thermochromic and heat storage coating for adaptive de/anti-icing and thermal regulation. *Chem. Eng. J.* **2024**, *482*, 148837. [CrossRef]

210. Zhao, S.; Yuan, A.; Chen, X.; Lei, Y.; Fu, X.; Lei, J.; Jiang, L. Single-actuated and fully recyclable phase change materials enabled multiple thermochromism toward information storage and encryption. *Chem. Eng. J.* **2024**, *481*, 148698. [CrossRef]
211. Cheng, Z.; Zhao, B.; Lei, L.; Zhu, Y.; Wei, Z.; Yu, T.; Fan, J.; Li, Y. Self-assembled poly(lactic acid) films with high heat resistance and multi-stage thermochromic properties prepared by blown film-annealing. *Chem. Eng. J.* **2024**, *480*, 148261. [CrossRef]
212. Tanioku, C.; Matsukawa, K.; Matsumoto, A. Thermochromism and structural change in polydiacetylenes including carboxy and 4-carboxyphenyl groups as the intermolecular hydrogen bond linkages in the side chain. *ACS Appl. Mater. Interfaces* **2013**, *5*, 940–948. [CrossRef]
213. Zhang, W.; Xu, H.; Chen, Y.; Cheng, S.; Fan, L.-J. Polydiacetylene-polymethylmethacrylate/graphene composites as one-shot, visually observable, and semiquantative electrical current sensing materials. *ACS Appl. Mater. Interfaces* **2013**, *5*, 4603–4606. [CrossRef] [PubMed]
214. Wang, M.; Wang, F.; Wang, Y.; Zhang, W.; Chen, X. Polydiacetylene-based sensor for highly sensitive and selective Pb^{2+} detection. *Dye. Pigment.* **2015**, *120*, 307–313. [CrossRef]
215. Wen, J.T.; Bohorquez, K.; Tsutsui, H. Polydiacetylene-coated polyvinylidene fluoride strip aptasensor for colorimetric detection of zinc (II). *Sens. Actuators B Chem.* **2016**, *232*, 313–317. [CrossRef]
216. Wang, D.-E.; Gao, X.; Li, G.; Xue, T.; Yang, H.; Xu, H. Facile colorimetric assay of alkaline phosphatase activity using polydiacetylene liposomes with calcium ions and pyrophosphate. *Sens. Actuators B Chem.* **2019**, *289*, 85–92. [CrossRef]
217. Dong, W.; Lin, G.; Wang, H.; Lu, W. New dendritic polydiacetylene sensor with good reversible thermochromic ability in aqueous solution and solid film. *ACS Appl. Mater. Interfaces* **2017**, *9*, 11918–11923. [CrossRef]
218. Qian, X.; Städler, B. Recent developments in polydiacetylene-based sensors. *Chem. Mater.* **2019**, *31*, 1196–1222. [CrossRef]
219. Lee, J.; Seo, S.; Kim, J. Biomolecule-Functionalized Smart Polydiacetylene for Biomedical and Environmental Sensing. *Molecules* **2018**, *23*, 107. [CrossRef]
220. Shi, Q.; Li, M.; Gong, K.; Zhao, Z.; Liu, D.; Zhou, X. Stable low temperature reversible thermochromic indicators for vaccine storage and transportation. *Dye. Pigment.* **2025**, *241*, 112894. [CrossRef]
221. Gouda, M.; Khalaf, M.M.; Abou Taleb, M.F.; Al Ghamdi, H.S.; Abd El-Lateef, H.M. Fabrication of Cellulose Nanofiber-Reinforced Polylactic Acid Nanocomposite Containing Anthocyanidin-Based Red Cabbage Extract for Anti-counterfeiting Thermochromic Ink. *Fibers Polym.* **2024**, *25*, 4885–4897. [CrossRef]
222. Guo, Y.; Hu, Z.; Zhan, L.; Liu, Y.; Sun, L.; Ma, Y. Stretchable Thermochromic Fluorescent Fibers Based on Self-Crystallinity Phase Change for Smart Wearable Displays. *Polymers* **2024**, *16*, 3575. [CrossRef] [PubMed]
223. He, Y.; Li, W.; Han, N.; Wang, J.; Zhang, X. Facile flexible reversible thermochromic membranes based on micro/nanoencapsulated phase change materials for wearable temperature sensor. *Appl. Energy* **2019**, *247*, 615–629. [CrossRef]

Disclaimer/Publisher's Note: The statements, opinions and data contained in all publications are solely those of the individual author(s) and contributor(s) and not of MDPI and/or the editor(s). MDPI and/or the editor(s) disclaim responsibility for any injury to people or property resulting from any ideas, methods, instructions or products referred to in the content.